NeuroImage 147 (2017) 934–951

Contents lists available at ScienceDirect

NeuroImage

journal homepage: www.elsevier.com/locate/neuroimage

Analysing concurrent transcranial magnetic stimulation and electroencephalographic data: A review and introduction to the open-source TESA software

Nigel C. Rogasch[a,*], Caley Sullivan[b], Richard H. Thomson[b], Nathan S. Rose[c], Neil W. Bailey[b], Paul B. Fitzgerald[b], Faranak Farzan[d], Julio C. Hernandez-Pavon[e]

[a] Brain and Mental Health Laboratory, School of Psychological Sciences and Monash Biomedical Imaging, Monash Institute of Cognitive and Clinical Neuroscience, Monash University, Australia
[b] Monash Alfred Psychiatry Research Centre, Central Clinical School, Monash University, Australia
[c] Department of Psychology, University of Notre Dame, USA
[d] Temerty Centre for Therapeutic Brain Intervention, Centre for Addiction and Mental Health, University of Toronto, Canada
[e] Department of Neuroscience and Biomedical Engineering, Aalto University School of Science, Espoo, Finland

ARTICLE INFO

Keywords:
Transcranial magnetic stimulation
Electroencephalography
EEGLAB
Artifacts

ABSTRACT

The concurrent use of transcranial magnetic stimulation with electroencephalography (TMS–EEG) is growing in popularity as a method for assessing various cortical properties such as excitability, oscillations and connectivity. However, this combination of methods is technically challenging, resulting in artifacts both during recording and following typical EEG analysis methods, which can distort the underlying neural signal. In this article, we review the causes of artifacts in EEG recordings resulting from TMS, as well as artifacts introduced during analysis (e.g. as the result of filtering over high-frequency, large amplitude artifacts). We then discuss methods for removing artifacts, and ways of designing pipelines to minimise analysis-related artifacts. Finally, we introduce the TMS–EEG signal analyser (TESA), an open-source extension for EEGLAB, which includes functions that are specific for TMS–EEG analysis, such as removing and interpolating the TMS pulse artifact, removing and minimising TMS-evoked muscle activity, and analysing TMS-evoked potentials. The aims of TESA are to provide users with easy access to current TMS–EEG analysis methods and to encourage direct comparisons of these methods and pipelines. It is hoped that providing open-source functions will aid in both improving and standardising analysis across the field of TMS–EEG research.

Introduction

Concurrent transcranial magnetic stimulation (TMS) and electroencephalography (EEG) is emerging as an important tool for assessing cortical properties such as excitation/inhibition, intrinsic oscillatory activity and connectivity (Bergmann et al., 2016; Ilmoniemi et al., 1997; Rogasch and Fitzgerald, 2013; Siebner et al., 2009). However, the combination of these modalities is technically challenging, resulting in several artifacts which severely distort the underlying neural signal of interest (Ilmoniemi et al., 2015; Ilmoniemi and Kičić, 2010). These artifacts present considerable problems for both interpreting and analysing TMS-evoked neural activity. In addition, typically used EEG analysis steps (e.g. filtering) in the presence of certain TMS-evoked artifacts can result in additional analysis-related artifacts, which further distort the signal of interest. In recent years, several approaches have been developed to either minimise or remove different artifactual signals, thereby allowing a more accurate assessment of TMS-evoked neural activity (Hernandez-Pavon et al., 2012; Korhonen et al., 2011; Mäki and Ilmoniemi, 2011). In addition to methods for removing artifacts, pipelines have also been suggested which minimise the introduction of analysis-related artifacts (e.g. Herring et al., 2015; Rogasch et al., 2014). The order of the processing steps within these pipelines necessarily departs from pipelines more commonly used in EEG research (e.g. Luck, 2005). Although descriptions of these pipelines have been published, the rapidly evolving field of TMS–EEG analysis can create challenges for those who are not familiar or skilled in scripting/coding, as many steps required for TMS–EEG analysis are not available in the majority of EEG analysis software. Therefore, open-source and easy-to-use analysis approaches are required for the TMS–EEG research community.

* Correspondence to: Brain and Mental Health Laboratory, Monash Biomedical Imaging, Building 220, Monash University, Melbourne, Victoria 3800, Australia.
E-mail address: nigel.rogasch@monash.edu (N.C. Rogasch).

http://dx.doi.org/10.1016/j.neuroimage.2016.10.031
Received 17 June 2016; Received in revised form 16 September 2016; Accepted 18 October 2016
Available online 20 October 2016
1053-8119/

To address the need for open-source TMS–EEG analysis, we introduce an extension called the TMS–EEG signal analyser (TESA), which is implemented in the open-source EEG analysis software EEGLAB (Delorme and Makeig, 2004) on the Matlab platform (Mathworks). The aim of TESA is two-fold. The first aim is to allow researchers without a scripting/coding background to learn and perform TMS–EEG analysis. To this end, TESA provides a series of functions that are accessible through the EEGLAB graphical user interface (GUI), and therefore do not require any coding experience. Most of these functions are specific to TMS–EEG analysis and are not found in most commercial EEG analysis software. The EEGLAB GUI has been used as it is helpful for learning how to develop scripted EEG analysis pipelines by storing examples of the called functions in the EEG structure, and by the considerable support available through the EEGLAB community. The GUI functionality both compliments and extends other open-source TMS–EEG analysis software, such as that available through the FieldTrip toolbox (Oostenveld et al., 2011). The second aim is to create a repository of methods for removing or minimising artifacts associated with TMS–EEG (e.g. TMS-evoked muscle activity). Removing TMS and physiological artifacts while minimising distortion of underlying neural activity is a non-trivial problem for the analysis and interpretation of TMS–EEG data. TESA includes several different approaches specifically designed to address this problem. The evidence for the effectiveness of these methods is varied. It is hoped that providing open access to these techniques will facilitate comparisons between methods and accelerate the development of validated approaches for successfully removing artifacts from TMS–EEG recordings. Furthermore, providing an open-source option for performing TMS–EEG analysis will improve consistency across the field.

In this paper, we first review the origins of artifacts in EEG recordings resulting from TMS. We also discuss the benefits and costs of various different methods used for removing/minimising certain TMS-evoked artifacts, such as those resulting from muscle activity. We then describe additional artifacts introduced by common EEG analysis steps, such as filtering and independent component analysis (ICA), and describe how these can be avoided by appropriate pipeline design. Finally, we introduce the functions included in TESA and provide a brief background for each type of analysis.

Artifacts in EEG recordings following TMS

The large magnetic field generated by TMS results in various different types of artifacts in EEG recordings. We define an artifact as any signal that is not the signal of interest (in this case TMS-evoked neural activity is the signal of interest). These artifacts can result from interaction between the magnetic field and the recording equipment (TMS pulse artifact, capacitor recharge artifact or electrical charge artifacts) or from the unintended, but inevitable, activation of physiological systems (TMS-evoked muscle artifacts, TMS-evoked sensory artifacts, eye blinks and/or movements, or persistent muscle activity resulting from jaw clenching/facial expressions). Each type of artifact requires different approaches for removal/minimisation. Some of these artifacts can be minimised or prevented online by appropriate experimental arrangements, whereas other require offline removal. In the following section, we provide an overview of the different types of EEG artifacts resulting from TMS and introduce methods used to remove/minimise these artifacts. For detailed mathematical descriptions of these methods, readers are directed to the original papers. Several other reviews also cover artifacts associated with TMS–EEG recordings and methods for removal and are recommended for additional reading (Ilmoniemi et al., 2015; Vernet et al., 2014).

Example data

Throughout the paper, examples of TMS–EEG artifacts and methods for analysing TMS–EEG data are given from a single individual. This example data is available for download from the following website. (https://figshare.com/articles/TESA_example_data_and_scripts/3188800). The example data was collected from a healthy participant as part of a project approved by the local Ethics Committee of the Medical Faculty of the Eberhard-Karls University Tübingen, Germany. Monophasic TMS pulses (current flow=posterior-anterior in brain) were given through a figure-of-eight coil (external diameter=90 mm) connected to a Magstim 200^2 unit (Magstim company, UK). Note that artifacts and analysis results are similar following biphasic stimulation, although monophasic pulses can result in larger decay artifacts and small offsets which persist following the pulse (Rogasch et al., 2013). 150 TMS pulses were delivered over the left superior parietal cortex (MNI coordinates: −20, −65, 65) at a rate of 0.2 Hz ± 25% jitter. The TMS coil position was determined using frameless stereotaxic neuronavigation (Localite TMS Navigator, Localite, Germany) and intensity was set at resting motor threshold of the first dorsal interosseous muscle (68% maximum stimulator output). EEG was recorded from 62 TMS-specialised, c-ring slit electrodes (EASYCAP, Germany) using a TMS-compatible EEG amplifier (BrainAmp DC, BrainProducts GmbH, Germany). Data from all channels were referenced to the FCz electrode online with the AFz electrode serving as the common ground. EEG signals were digitised at 5 kHz (filtering: DC-1000 Hz) and EEG electrode impedance was kept below 5 kΩ. All offline analysis was performed in Matlab 2015b (Mathworks, USA) using the open-source toolbox EEGLAB (Delorme and Makeig, 2004) and the TMS–EEG signal analyser (TESA) extension introduced in this paper. Raw EEG data was epoched around the TMS pulse (−1000 to 1000 ms). Data were then manually inspected and trials with large bursts of muscle activity (e.g. from jaw clenching; ~50 μV or larger) were removed (8 trials), as were electrodes that became disconnected during recording (3 electrodes).

TMS pulse artifact

The large (up to 3 T), but brief (~200 μs) time-varying magnetic field surrounding the coil following TMS discharge causes a very large spike artifact in the EEG recording (4–5 orders of magnitude larger than neural activity). This artifact saturated older generation EEG amplifiers (e.g. amplifiers manufactured prior to 2000), resulting in a slow recovery of the EEG signal (hundreds of ms), severely limiting concurrent TMS–EEG research (Amassian et al., 1992; Cracco et al., 1989; Izumi et al., 1997). Two main approaches have been adopted to cope with the TMS pulse artifact. First, a sample-and-hold circuit was developed which isolates and pins the amplifier for a short time (2–10 ms) around the TMS pulse, preventing recording of the TMS pulse artifact (Ilmoniemi et al., 1997; Virtanen et al., 1999). The second approach resulted from improved EEG amplifier hardware, which included direct current (DC)-coupling (as opposed to alternating current) and increased sampling rates (> 5 kHz), bit resolution (≤24 nV/bit) and recording ranges (> 300 mV) (Bonato et al., 2006; Daskalakis et al., 2008; Fitzgerald et al., 2008; Veniero et al., 2009). The improved sampling capabilities of these EEG amplifiers prevent saturation, resulting in a large pulse or 'ringing' artifact, which reflects the step response of the amplifiers (Fig. 1A). Preventing saturation allows the EEG signal to return to baseline levels within 5–10 ms of the TMS pulse under optimised recording conditions (see below; Rogasch et al., 2013; Veniero et al., 2009). The most common method for eliminating the TMS pulse artifact is to remove the affected data and replace it with either linear or cubic interpolation (Bergmann et al., 2012; Thut et al., 2011). Cubic interpolation is useful for minimising sharp transition edges which can interact with filters. Note that for large amplitude changes in the data, such as those occurring from TMS-evoked muscle activity, cubic interpolation can be improved by fitting smaller amounts of data around the artifact. If a cubic function cannot adequately model the data, linear interpolation can also be used, but may result in high frequency edges.

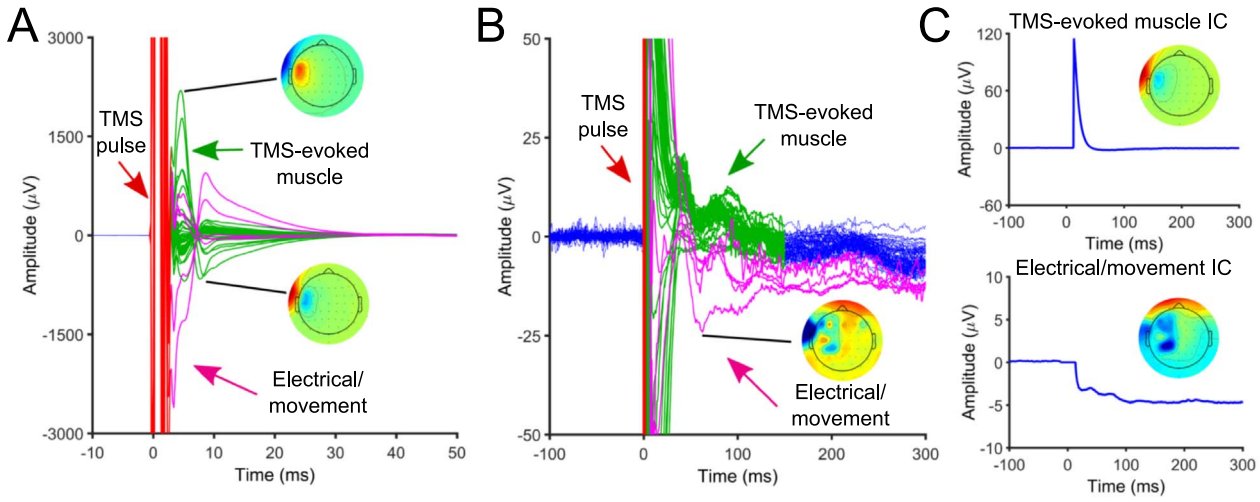

Fig. 1. Artifacts in electroencephalographic (EEG) signals resulting from single transcranial magnetic stimulation (TMS) pulses. A) Raw TMS-evoked EEG activity from all electrodes averaged across trials following epoching and baseline correction. Several major artifacts are present including the TMS pulse artifact (red), the TMS-evoked muscle artifact (green) and an offset/decay artifact possibly resulting from stored electrical charges or electrode movement (magenta). Topoplots show the peaks of the TMS-evoked muscle activity at ~5 and 8 ms. B) Expanded view of TMS-evoked activity showing the different artifacts. Note that offset electrodes (demonstrated by topoplot) gradually decay towards zero over ~1.5 s. C) Independent components (ICs) extracted following FastICA. Data around the TMS-pulse and peaks of the TMS-evoked muscle artifact were removed and replaced with constant amplitude data prior to FastICA. Note the TMS-evoked muscle artifact and electrical/movement artifact are captured in separate components, despite a similar topography. (For interpretation of the references to color in this figure legend, the reader is referred to the web version of this article.)

Capacitor recharge artifact

Following a TMS pulse, the capacitors which store the electrical charge required for TMS are recharged. The recharging can result in additional artifacts, particularly in electrodes either in contact or close to the TMS coil. This artifact can either appear as another small spike following the TMS pulse (Magstim stimulators; Veniero et al., 2009), or a step followed by an exponential decay (MagVenture stimulators; Rogasch et al., 2013). For Magstim stimulators, the timing of this recharge following the TMS pulse is dependent on the intensity of stimulator output, meaning the timing of this artifact can vary depending on individual participants (Veniero et al., 2009). For MagVenture stimulators, the timing of the capacitor recharge can be manually determined (Rogasch et al., 2013). Note that the recharge artifact is considerably less severe in newer generation MagVenture and PowerMag stimulators (MAG and More), provided the electrode impedance is low and the electrode lead wires optimally arranged. As with the TMS pulse artifact, the capacitor recharge artifact is usually removed and missing data replaced with interpolated data. Alternatively, short spike recharge artifacts can be removed using a median filter (Rose et al; In press).

TMS-evoked muscle artifacts

TMS not only stimulates underlying brain tissue, but any tissue with high conductance (e.g. muscles, peripheral nerves) in the vicinity of the coil. TMS can either directly stimulate facial/scalp muscles or can activate these muscles by stimulating the motor neurons innervating the muscles. This stimulation results in a compound muscle action potential, which is recorded as a biphasic signal with peaks at 4–5 and 7–10 ms in electrodes ipsilateral to the stimulated hemisphere (Fig. 1A–B) (Mutanen et al., 2013; Rogasch et al., 2013). Note that the exact timing of the peaks is dependent on the sampling rate and filter settings, with lower rates delaying the muscle peaks, and in some instances causing the early peak to mix with the TMS pulse artifact. The appearance of this TMS-evoked muscle artifact is similar to responses recorded from peripheral muscles, such as an M-wave following peripheral nerve stimulation or a motor-evoked potential recorded following TMS to the motor cortex, with amplitudes > 1 mV (Korhonen et al., 2011; Mutanen et al., 2013; Rogasch et al., 2013). This contrasts with muscle activity observed following jaw clenching or facial expression, which appears as either ongoing or short bursts of high frequency signal (see Fig. 2). The tail of TMS-evoked muscle activity appears as an exponential decay-shaped signal and can take > 50 ms to recover, offsetting the underlying neural signal. Stimulation of scalp muscles can be reduced by positioning the coil close to the mid-line, using focal TMS coils and using lower TMS intensities (Massimini et al., 2005; Mutanen et al., 2013; Rogasch et al., 2013).

Electrical artifacts

The magnetic field generated by the TMS pulse interacts with skin-gel-electrode interface (Julkunen et al., 2008), the electrodes (Virtanen et al., 1999), and the electrode lead wires (Sekiguchi et al., 2011), resulting in the accumulation of electrical charges. These interactions can cause large initial deflections in voltage which decay over time, resulting in lasting offsets in the EEG signal. The decay artifacts resulting from electrical charges tend to be largest in electrodes near the coil, and last anywhere between 5 milliseconds to several seconds (Fig. 1). Such artifacts can be minimised online with careful EEG preparation including reducing the electrode impedance as much as possible (< 5 kΩ), using TMS-compatible EEG electrodes (e.g. sintered Ag-AgCl pellet electrodes, C-ring slit electrodes), and arranging the electrode lead wires perpendicular to the TMS coil handle to maximise common-mode rejection of the artifacts (Julkunen et al., 2008; Sekiguchi et al., 2011). When using DC-coupled amplifiers with optimal preparation, the majority of these decay artifacts recover within 5–10 ms (Rogasch et al., 2013; Veniero et al., 2009), however small offsets might persist under certain conditions (e.g. following monophasic pulses).

Electrode movement artifacts

Movement artifacts resulting from electrode displacement following TMS-evoked muscle twitches at the scalp can also occur (Rogasch et al., 2014), and can be reduced by avoiding stimulation of scalp muscles. Electrode displacement can also occur from the pressure of holding the TMS against an electrode. This can be minimised by placing a thin layer of foam between the coil and electrode.

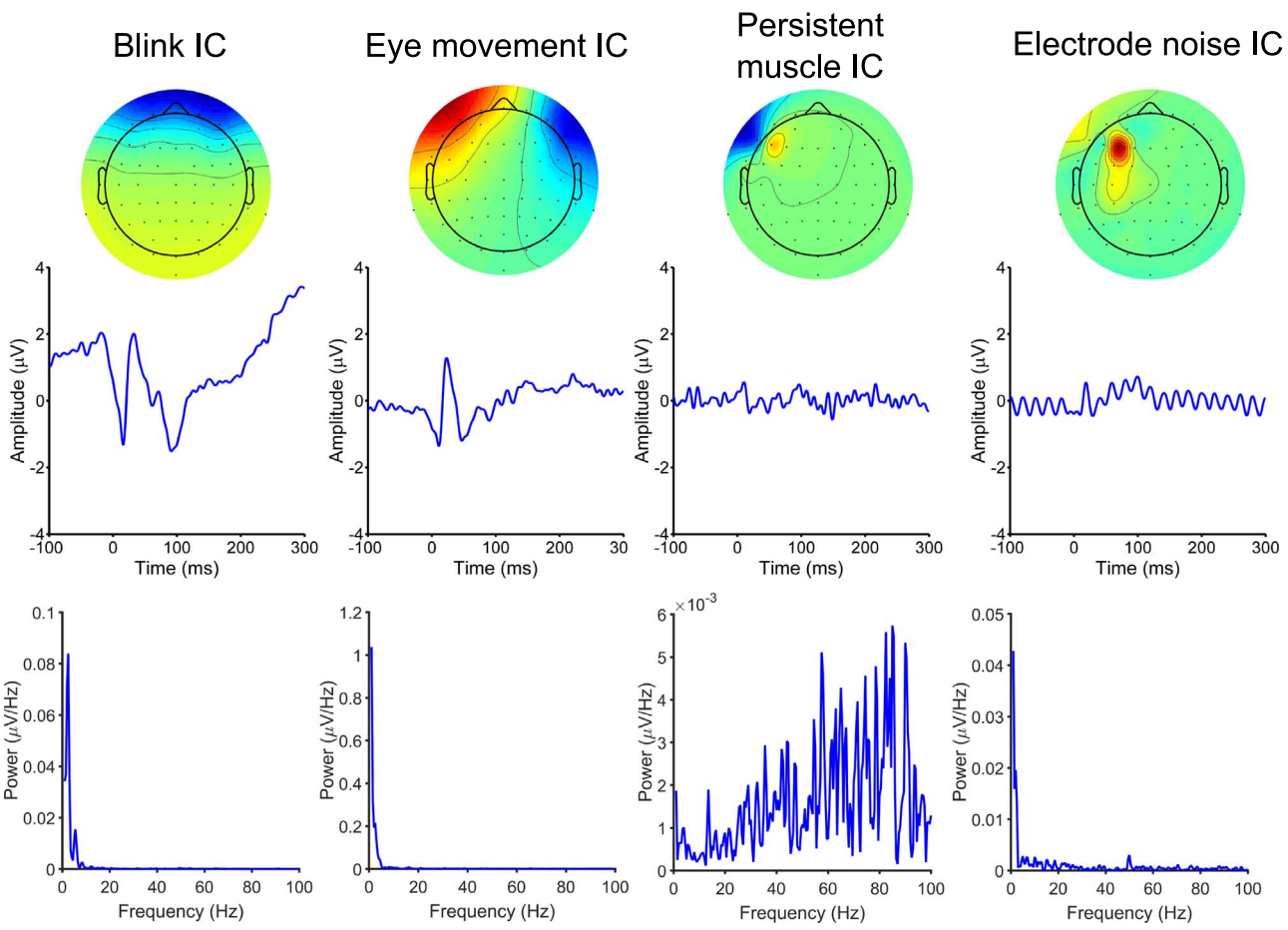

Fig. 2. Other common electroencephalographic (EEG) artifacts observed in concurrent transcranial magnetic stimulation (TMS) recordings**.** Independent components (ICs) extracted following FastICA representing other types of artifacts present in TMS–EEG signals. Artifacts include blinks, horizontal eye movements, persistent muscle activity and line noise. The top panel shows the topographic representation of the IC, the middle panel the time course, and the bottom panel the frequency distribution of the time course. Note that the TMS pulse and peaks of the TMS-evoked muscle activity (−12 to 12 ms) were removed prior to FastICA.

Removing TMS-evoked muscle, electrical, and movement artifacts offline

Although preventing the large, early artifacts by optimising the experimental arrangement is preferable, especially for minimising electrical artifacts, this may not be possible for all experimental arrangements. For example, the brain region of interest in the study might lie underneath scalp muscles, (e.g. dorsolateral prefrontal cortex, Broca's area), making it impossible to avoid TMS-evoked scalp muscle artifacts. Given that the TMS-evoked neural activity of interest occurs within the first 300 ms following the TMS pulse, several offline approaches have been developed to remove these artifacts. However, accurately recovering the neural signal underlying such large amplitude artifacts (possibly >1000 μV in amplitude) has proven challenging, and is currently an active area of research. Here, we provide a brief overview of the different approaches developed to remove/minimise TMS-evoked muscle, electrical, and movement artifacts. In practice, it can be difficult to differentiate these artifacts as each results in a decay-shaped signal (e.g. Fig. 1). Accordingly, many papers do not make a clear distinction between which type of artifact is being removed. However, most methods should be suitable for any large amplitude artifact, which decays over time.

Principal component analysis (PCA)

PCA is a blind source separation method that finds scalp topographies representing the maximally orthogonalised signal from EEG data (i.e. scalp topographies with maximal difference). As such, signals with different origins (artifacts and neural signal) are represented in different components. PCA can be used to directly suppress/minimise the TMS-evoked muscle artifact in a process called PCA suppression (Hernandez-Pavon et al., 2012). In this approach, PCA is applied to the data period directly relevant to the TMS-evoked muscle artifact (e.g. ~10 to 40 ms coinciding with the tail of the artifact). The principal components best capturing the artifact, usually 1–5 of the top components, are suppressed before the mixing matrix is applied back to the full dataset, thereby removing the artifact from the data (Hernandez-Pavon et al., 2012).

PCA has also been used as a pre-processing step to aid in the decomposition of independent component analysis (ICA; see below). PCA can be used to reduce the rank or dimensionality of the data to better estimate the true number of neural and artifact components contained within the signal. This is also referred to as “truncating” or “compressing” the data (Hernandez-Pavon et al., 2012; Korhonen et al., 2011). As with independent components, individual principal components explain differing amounts of variance in the data, with the first principal component explaining the most variance. The distribution of variance explained by principal components is typically captured by a power law, meaning that a small number of principal components account for most of the variance in the data. Compression is achieved by only retaining the principal components that represent the majority of the data (e.g. the top 25–30 of 60 principal components in a 60 electrode recording), making the assumption that the removed principal components represent noise. The rationale for performing a compression step is to prevent over-fitting of the ICA and therefore splitting of components representing a single origin (e.g. blinks or a

neural signal) into multiple components. However, an accurate estimate of the number of underlying sources is required to optimally use PCA, which is generally unknown for EEG signals. Therefore, the use of PCA for compression prior to ICA will shift the risk from over-fitting to under-fitting (i.e. mixing signals from multiple single origins in to one component). The most appropriate number of components required for accurate retrieval of TMS-evoked neural activity requires further research. Alternatively, in a similar method to that presented by Korhonen et al. (2011) and Hernandez-Pavon et al. (2012), PCA compression can also be applied to remove the muscle artifacts (ter Braack et al., 2013).

Multiple-source artifact correction and signal space projection

Several methods related to PCA have also been suggested to remove large artifacts in TMS–EEG data. Litvak et al. (2007) adapted an artifact correction approach originally designed to correct eye blink/movement artifacts, which uses scalp topographies and source analysis to remove artifacts from neural signal (Berg and Scherg, 1994). In this approach implemented in the BESA software, a source model is constructed which consists of both artifact and brain topographies. A linear inverse operator is then constructed from this source model, and the data is decomposed into a linear combination of artifact and neural signals. The artifact signals can then be subtracted from the data. For TMS–EEG data, the artifact topographies were estimated by applying PCA to the early signal primarily represented by the early TMS-evoked muscle and electrical artifacts (< 15 ms). Brain topographies were estimated using multiple dipole source analysis. Using these estimated topographies, the artifact subtraction process was repeated iteratively, initially using the first PC (which is most likely to represent the TMS-evoked artifacts) in the artifact model, and then adding additional PCs until these artifacts were adequately removed, leaving just the neural signal (Litvak et al., 2007). Maki and Ilmoniemi (2011) adopted a related approach to remove the TMS-evoked muscle artifact called signal-space projection. This approach estimates the signal sub-space containing the artifact and uses a linear operator to remove the artifact from the measured signal (Uusitalo and Ilmoniemi, 1997). To estimate the signal subspace containing the artifact, the authors first low-pass filtered the signal to 100 Hz, arguing that muscle activity is typically higher frequency than neural activity. The muscle topographies were then estimated using PCA, and projected out using signal-space projection from the broad band data (Mäki and Ilmoniemi, 2011). A limitation of this method is that signal around the site of stimulation was highly attenuated. To overcome this limitation, Mutanen et al. (2016) recently introduced a second step to this analysis called source-informed reconstruction. Following artifact removal using signal-space projection, the data are projected in to source space using minimum-norm estimates and then re-projected on to the scalp surface using the lead-field matrix and estimated sources (Mutanen et al., 2016). This approach overcomes the signal attenuation associated with signal-space projection alone, and results in TMS-evoked potentials consistent with activity from the stimulated cortical region as early as 15 ms following TMS. However, some localised distortion of neural sources radial to the removed artifact was observed.

Independent component analysis(ICA)

ICA is another blind source separation technique used to separate out statistically independent components from linearly mixed signals, such as artifacts and neural signal in EEG recordings (Hyvärinen and Oja, 2000; Makeig et al., 1997). Whereas PCA finds scalp topographies with maximal difference, ICA finds temporally independent components that could be non-orthogonal (i.e. have scalp distributions that are very similar). Following separation, the independent components representing artifacts can be subtracted before the signal is re-calculated, hence removing the artifacts. ICA is commonly used to remove eye movement and persistent muscle activity from regular EEG recordings and several papers have extended this use to remove TMS-evoked muscle, electrical and movement artifacts (Hamidi et al., 2010; Korhonen et al., 2011; Rogasch et al., 2014). Indeed, FastICA may be able to separate different types of large artifacts which occur over different time scales and have slightly different topographies, such as the tail of TMS-evoked muscle activity, electrical charges and electrode movement (Rogasch et al., 2014; Fig. 1C). The main assumption in using ICA for TMS–EEG data is that artifacts are temporally independent of neural signal. Another assumption is that the topographies of large amplitude components are not as susceptible to distortion as smaller components, which can affect decomposition accuracy (for further discussion see *Distortion of ICA resulting from TMS-evoked muscle activity*). Several different types of ICA algorithm exist and both FastICA (Hyvärinen and Oja, 2000) and infomax (Makeig et al., 1997) algorithms are commonly used for TMS–EEG analysis. There is still some debate as to which algorithm is most appropriate for EEG analysis (Delorme et al., 2012); however, this discussion is beyond the scope of the current paper.

Enhanced deflation method(EDM)

An alternative FastICA method for removing the TMS-evoked muscle artifact is the enhanced deflation method (EDM) introduced by Korhonen and colleagues (2011). This approach overcomes the instability of the FastICA deflation method by running the fixed-point algorithm multiple times and sorting the components with the highest negentropy (e.g. highest organisation). The independent components with the highest negentropy typically represent the TMS-evoked muscle activity and can be removed semi-automatically (Korhonen et al., 2011).

Detrending data

An alternate approach for removing decay shaped artifacts, especially those related to electrical charges, is to “detrend” the data by fitting a model to the artifact (e.g. a linear or exponential function) and then subtracting the modelled data from the overall signal (Verhagen et al., 2012). The assumption underlying this approach is that any consequent decay artifacts resulting from stored electrical charges, muscle activity or electrode movement are well explained by these functions, and the TMS-evoked neural activity is linearly superimposed on to the artifactual activity. Note that the peaks of the TMS pulse and TMS-evoked muscle activity need to be removed prior to using this technique.

Filtering

As discussed below (see *Artifacts introduced to TMS–EEG recordings during analysis*), conventional filtering approaches can interact with the TMS pulse and large amplitude artifacts to introduce additional artifacts, and are therefore not recommended. However, more advanced filters capable of modelling the non-stationary components of the TMS–EEG signal, such as Kalman filters, have been adopted to remove electrical artifacts resulting from TMS (Morbidi et al., 2007). However, this approach has not been widely adopted.

Varying levels of evidence exist for the efficacy of the above methods in removing the large amplitude artifacts associated with TMS-evoked muscle activity, electrical charges, and electrode movement, while maintaining underlying neural activity. A major issue in evaluating the efficacy of these methods is generating an appropriate “ground truth” to compare against (i.e. a known neural signal that is masked by the TMS-evoked artifacts such as muscle activity). One approach to this problem is to simulate the time course and location of a neural signal and then add this simulated data to actual TMS–EEG data prior to pre-processing. The success in retrieving both the time course and

topography of the known simulated signal is then evaluated following artifact removal. Such an approach was used to evaluate and compare methods of PCA suppression in data with large artifacts (Hernandez-Pavon et al., 2012). Following PCA compression, both PCA suppression alone and PCA suppression with wavelet filtering (similar to signal-space projection) were able to accurately retrieve neural signal either at the site of stimulation or a remote site between 15–40 ms following the TMS pulse. However, both methods performed less accurately when the neural signal was closer to the pulse (10–35 ms) due to the strong artifacts evoked from Broca's area stimulation. Signal-space projection combined with source-informed reconstruction has also been compared against a simulated source in the brain region receiving TMS (motor cortex), and appears capable of retrieving neural signal as early as 15 ms following TMS (Mutanen et al., 2016); however, the artifacts were of moderate size. FastICA is able to greatly suppress decay artifacts, resulting in a similar cleaned signal to PCA suppression (Rogasch et al., 2014). However, the ability of FastICA to accurately retrieve underlying neural activity has not been directly quantified with simulated data as of yet. Methods such as multiple-source artifact correction, detrending and Kalman filtering all significantly reduce the size of large amplitude artifacts; however these approaches have yet to be tested against the blind source separation methods, or against simulated data. Further research directly comparing the ability of these different methods to accurately recover TMS-evoked neural activity in the presence of large muscle artifacts is required to decide most appropriate approach to use.

TMS-evoked sensory artifacts

The TMS pulse activates the brain both directly via the induced electrical current (intended) and indirectly by interaction with the sensory systems (unintended, but inevitable). TMS discharge is accompanied by a loud click which results in an auditory-evoked potential with two major peaks around 100 and 200 ms following the pulse (Nikouline et al., 1999; Tiitinen et al., 1999). The TMS pulse also activates the somatosensory system, most likely by stimulating scalp muscles or afferent nerve fibres running across the scalp (i.e. the tapping sensation felt when given TMS). The evoked potential resulting from somatosensory input occurs contralateral to the site of TMS stimulation (Paus et al., 2001) and also has central peaks around 100 and 200 ms (Herring et al., 2015). An additional somatosensory-evoked potential can occur when the motor cortex is stimulated above motor threshold, as TMS results in twitches of peripheral muscles that provides re-afferent sensory stimuli to the cortex. This movement-related somatosensory-evoked potential is likely time-shifted with the conduction delay between the cortex and periphery, beginning at approximately 50–60 ms following the TMS pulse (Paus et al., 2001; Spieser et al., 2010). The auditory-evoked potential can be minimised online by playing a masking noise through headphones (often white noise) and a layer of foam between the coil and head to prevent bone conducted components (Nikouline et al., 1999; Massimini et al., 2005; ter Braack et al., 2015). Offline approaches for minimising auditory-evoked potentials include subtracting the signal following sham stimulation (e.g. the click without active stimulation of the cortex) (Kähkönen et al., 2003) or using ICA (Rogasch et al., 2014). However, it remains unclear whether any of these methods are able to completely remove auditory–evoked activity. The somatosensory-evoked potential resulting from scalp muscle activation is much more difficult to prevent online and identify offline. The main approach for prevention is to stimulate with as low intensity as possible and to avoid stimulating scalp muscles (which is not possible for all experimental designs). No methods are currently available for offline removal of this somatosensory-evoked potential. For all kinds of sensory artifacts, an alternative to removing the artifact is to have good control conditions in which, for example, TMS is delivered at the same intensity to control regions, trial types, or time points within a trial that are not hypothesized to have the same effect as in the conditions of interest. This approach allows for the separation of alterations in TMS-evoked neural activity from sensory artifacts. Another solution is a test – manipulation – re-test experimental design, where stimulation site and parameters are held constant. In this design, changes in TMS-evoked activity can be safely ascribed to the experimental manipulation, as opposed to TMS-evoked sensory artifacts, which should remain constant.

Eye movement, persistent muscle activity, line noise, and other artifacts

Various other types of artifacts, which are common to all EEG experiments (Jung et al., 2001; Onton et al., 2006), also impact TMS–EEG recordings (Fig. 2). Eye movements (including larger horizontal and vertical movements and smaller microsaccades) and blinking can impact the EEG signal due to the strong corneo-retinal dipole (Plöchl et al., 2012). This can be particularly problematic for TMS–EEG recordings, as TMS can result in a time-locked reflex blink in some individuals, particularly when frontal sites are stimulated (Lyzhko et al., 2015; Rogasch et al., 2014). Jaw clenching, squinting and other facial expressions results in high-amplitude phasic or low-amplitude tonic muscle activity which impacts high-frequency signal (McMenamin et al., 2010). Line noise from electrical equipment can also interfere with recordings at either 50 or 60 Hz depending on the power line/mains frequency of the country. When these artifacts are infrequent, discarding affected data is the most common approach for offline removal. However, if the problem is more persistent, methods such as ICA, PCA, filtering (for artifacts listed in this section excluding eye-related artifacts), and regression analysis are also commonly used (Daskalakis et al., 2008; Litvak et al., 2007; Rogasch et al., 2014). A final consideration is the length of TMS–EEG testing sessions, which can last considerably longer than sessions with either TMS or EEG alone due to the considerable preparation and set up time. The session length can result in participant fatigue, which has the potential to substantially alter TMS-evoked neural activity (e.g. during the early stages of sleep; see Massimini et al., 2005).

Artifacts introduced to TMS–EEG recordings during analysis

Typical analysis pipelines for event-related potential EEG studies include several steps such as filtering, downsampling, epoching, baseline-correcting, ICA and finally averaging the data across epochs (Bigdely-Shamlo et al., 2015; Luck, 2005). The unique nature of certain artifacts in TMS–EEG recordings, such as the TMS pulse artifact and TMS-evoked muscle artifacts, have necessitated specialised analysis pipelines to remove artifacts without introducing unwanted distortions to the data. This has proven challenging due to the interaction of such artifacts with common cleaning procedures used in EEG analysis such as filtering and ICA.

Filtering artifacts resulting from the TMS pulse artifact

Filtering is typically applied either during acquisition or as a first step in analysis to remove unwanted low frequency drifts (high-pass filtering) and high-frequency noise (low-pass filtering) from EEG signal (Luck, 2005). Applying filters can be considered a controlled distortion of the data and, if used incorrectly, can introduce unexpected artifacts such as ringing or ripple artifacts, or distort the neural signal of interest (Acunzo et al., 2012; Tanner et al., 2015; VanRullen, 2011; Widmann et al., 2014; Widmann and Schröger, 2012). Ringing/ripple artifacts typically occur at sharp transitions in the data, for example at the boundaries of an epoch or following a large jump in the signal amplitude. The extremely large amplitude and high frequency nature of the TMS pulse artifact introduces ringing and drift artifacts following filtering (Fig. 3A). Therefore both online and offline filtering should be avoided until the TMS pulse artifact is removed. For amplifiers that

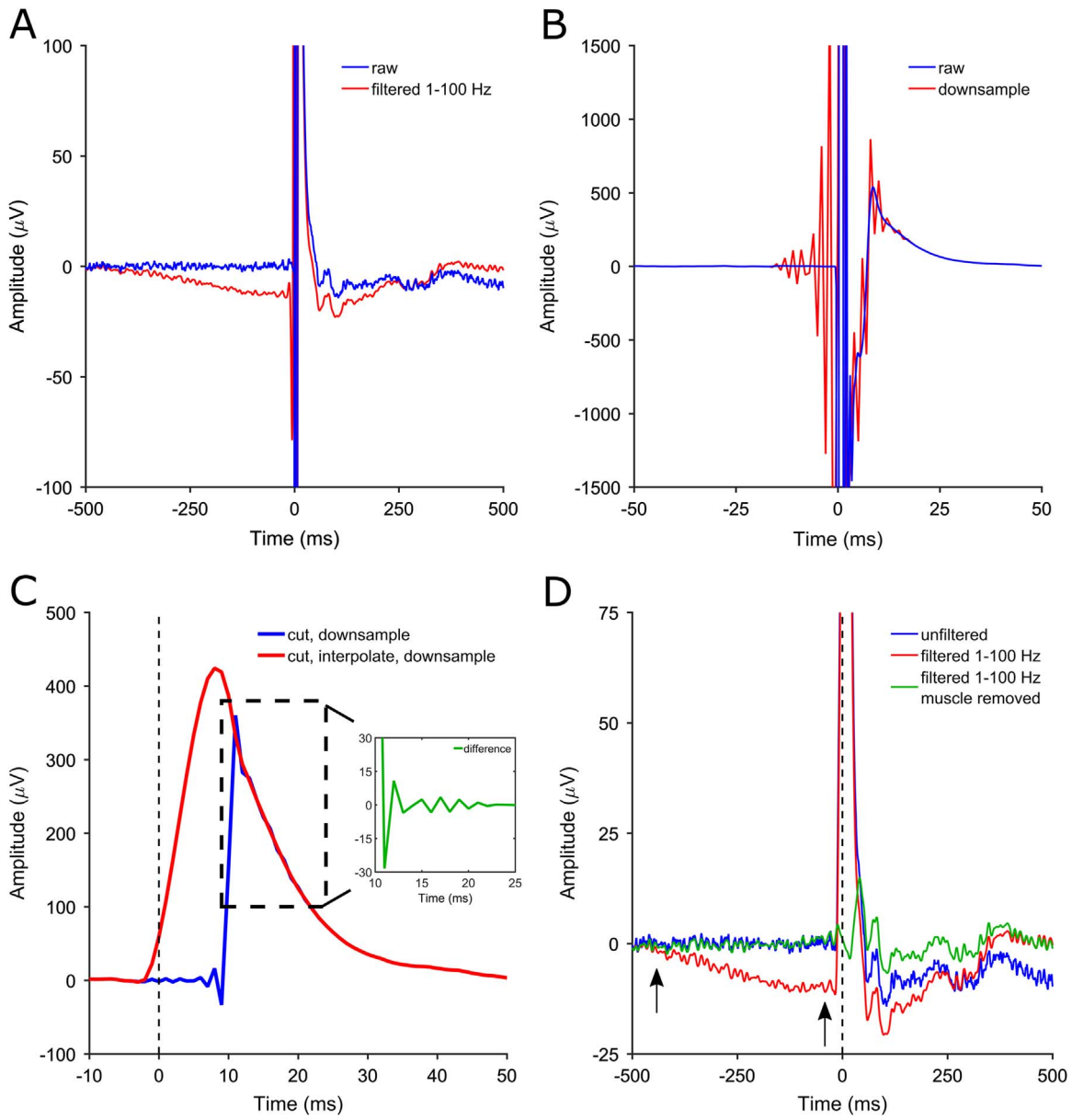

Fig. 3. Artifacts resulting from filtering. A) Raw and filtered (zero-phase, fourth order, band-pass Butterworth filter; 1–100 Hz) electroencephalographic (EEG) data from a single electrode (T7) following transcranial magnetic stimulation (TMS). The large amplitude and high frequency of the TMS pulse artifact result in drift and ringing artifacts following filtering, which alter TMS-evoked neural activity. B) Raw data and data following downsampling. An anti-aliasing low-pass filter is automatically applied using the *resample* EEGLAB function, which also results in a ringing artifact in the presence of the TMS pulse artifact (red trace); however, the duration is considerably shorter than with band-pass filtering (~ ± 20 ms recovery). C) The ringing artifact resulting from anti-aliasing filters can be minimised by removing the TMS pulse and peaks of the TMS-evoked muscle activity (between −2 and 10 ms). Data were either replaced by constant amplitude data equivalent to a sample-and-hold circuit (blue trace), or cubic interpolation (red trace; cubic window= ± 1 ms). Note that smaller amplitude ringing artifacts are still present for up to ~25 ms when removed data is replaced by constant amplitude data due to the large step in amplitude (evident from green inset graph which shows the difference between constant amplitude and cubic data). No ringing artifacts are observed following cubic interpolation. D) Unfiltered and filtered data (zero-phase, fourth order, band-pass Butterworth filter; 1–100 Hz) following downsampling and removal of TMS pulse artifact (−2 to 10 ms). Removed data has been replaced using cubic interpolation to minimise step artifacts. Removing the TMS pulse artifact minimises any ringing artifacts following filtering (e.g. compared to A); however, the large amplitude tail of the TMS-evoked muscle activity still results in a drift artifact (red trace; most obvious in pre-stimulus data due to zero-phase filter; indicated with arrows). This drift artifact can be prevented by removing/minimising the tail of the TMS-evoked muscle activity, in this case by subtracting the independent component representing the residual muscle activity following FastICA (green trace). (For interpretation of the references to color in this figure legend, the reader is referred to the web version of this article.)

attempt to capture and fully characterise the artifact, avoiding filtering during acquisition is particularly important. This can be achieved by using DC-coupling, which removes online high-pass filtering, and high sampling rates > 5000 Hz, which enables low-pass filters at least as high as 1000 Hz in most systems, a frequency sufficient to capture the artifact with fast recovery (< 10 ms) (Rogasch et al., 2013; Veniero et al., 2009). Here, the low-pass filter and sampling frequency are set to satisfy the Nyquist theorem, which states that sampling frequency must be at least twice the lowest frequency of interest in the signal. In practice, most amplifier systems impose a low-pass filter that is 4–5 times lower than the sampling frequency. DC-drift during DC-coupling recordings can result in 'clipping' of the TMS pulse artifact (e.g. when the signal is outside of the recording range of the amplifier), or even saturation of the signal in certain experimental arrangements. In the case of saturation, manual or automatically triggered DC-corrections at experimentally suitable times may be necessary. DC-drifts can be removed offline using software-based filters, provided certain TMS-related artifacts are adequately removed (see below).

Sampling the data at such high rates results in high-resolution data, and therefore large file sizes, which are usually well above that required

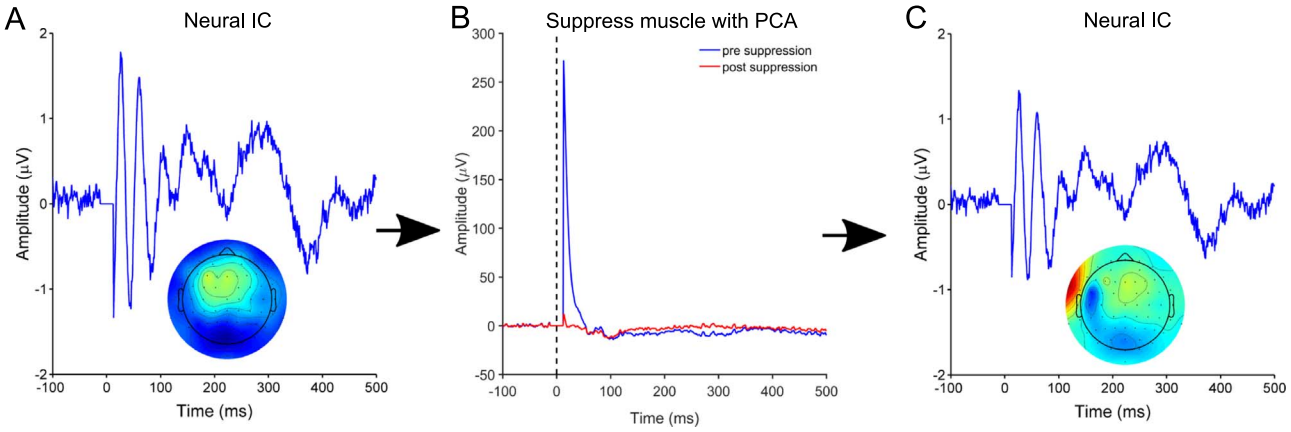

Fig. 4. Distortion of independent component (IC) topographies caused by large amplitude transcranial magnetic stimulation (TMS)-evoked muscle artifacts. A) An independent component (IC) likely representing neural activity following TMS. Prior to FastICA, data were downsampled and the TMS pulse and peaks of TMS-evoked muscle activity were removed (±12 ms). The dimensionality of the data was reduced to a rank of 25 using principal component compression (see Hernandez-Pavon et al. (2012) for details). B) Data from the T7 electrode showing the large amplitude tail of the remaining TMS-evoked muscle artifact (blue trace). The amplitude of this residual muscle activity was reduced to within the range of neural activity using principal component suppression (red trace; 1 PC removed). C) The same neural component from A after suppression of the muscle artifact. Note that the time course is nearly identical to that in A, however the topographies are different, with the new topography over lateral electrodes close to those affected by muscle. (For interpretation of the references to color in this figure legend, the reader is referred to the web version of this article.)

for the neural signal of interest. Due to these large file sizes, another common early step in analysis is to downsample the data to a more reasonable resolution (usually 500–1000 Hz). Downsampling can cause aliasing artifacts that introduce spurious signals in the data caused by the removal of data points. Aliasing can be avoided by applying a low–pass filter at half of the frequency (or lower) of the downsampled frequency resolution to satisfy the Nyquist theorem prior to downsampling (e.g. if downsampled to 1000 Hz a low–pass filter of 500 Hz is applied). It is important to note that some software automatically apply an anti-aliasing filter with downsampling, such as the EEGLAB *resample* function. In the presence of the TMS pulse artifact, low-pass anti-aliasing filters can also produce small ringing artifacts that increase in duration with larger reductions in sampling rate (Fig. 3B, red trace). The start and end of these artifacts can be easily identified by comparing the original signal with the down-sampled signal. To avoid/minimise ringing artifacts resulting from the anti-aliasing filters, large steps and steep gradients in the data need to be removed. This can be achieved by removing the TMS pulse artifact and the peaks of the TMS-evoked muscle artifact (e.g. −2 to 10 ms), and interpolating the missing data before downsampling (Fig. 3C, red trace). The success of avoiding ringing artifacts is dependent on both the cut-off frequency of the low pass filter (determined by the new sampling rate) and the steepness of the gradient between the real and interpolated data (determined by the size of any residual large amplitude artifacts). As such, data should be carefully examined following this step to ensure ringing has been minimised. As sharp edges and steps in the data need to be avoided, cubic interpolation is a good option. Note that for large amplitude artifacts, the performance of a cubic function is improved by limiting the data used for fitting to small windows around the edge of the removed signal (e.g. ±1 ms). If a cubic function fails to adequately model the large decay artifacts, linear interpolation is another option; however, this may result in a high frequency edges.

Filtering artifacts resulting from large amplitude artifacts

Even after the TMS pulse artifact and the large amplitude peaks of the TMS-evoked muscle artifact have been removed and the missing data interpolated, the residual decay artifacts (e.g. from the tail of the TMS-evoked muscle artifact and electrical charge artifacts) can still result in a high-amplitude step in the data which is problematic for band-pass filtering at frequencies regularly used for EEG analysis (e.g. 1–100 Hz). An example of the artifacts introduced by band-pass filtering in the presence of such artifacts can be seen in Fig. 3D (red trace). The slow drift artifact introduced by filtering is particularly obvious before the TMS pulse (note this reflects the zero-phase of the filter; the filter is applied forward, then backwards to prevent phase shifts). Therefore, it is important to also remove residual large amplitude artifacts before offline band-pass filtering. As the artifacts resulting from electrical decay artifacts can last several hundred milliseconds, simply removing this data will result in loss of the entire signal of interest and is therefore not a viable option. Minimising or removing these high-amplitude artifacts without distorting the underlying neural signal of interest is extremely challenging and several different methods have been suggested (as described in *Removing TMS-evoked muscle, electrical, and movement artifacts offline*).

Distortion of ICA resulting from large TMS-evoked muscle activity

Another potential problem in TMS–EEG analysis created by high-amplitude artifacts, such as the TMS-evoked muscle artifact from cranial areas, is weakening the ability of ICA to accurately uncover the neural EEG signal (Hernandez-Pavon et al., 2012). ICA is commonly used in EEG analysis to remove artifactual signals such as eye movements, low-level persistent muscle activity, line noise and is also used in TMS–EEG analysis to remove the TMS-evoked muscle activity of moderate size (Rogasch et al., 2014). However, EEG signals that are orders of magnitude larger than the neural signal of interest, such as those generated by TMS-evoked muscle activity of highly artifactual areas, can distort the spatial distribution of independent components representing neural signals (Fig. 4) (Hernandez-Pavon et al., 2012). Removal of distorted artifactual components will result in a “cleaned” signal with accurate temporal properties, but misleading spatial properties. Therefore, suppression of the high-amplitude, TMS-evoked muscle artifact with methods such as PCA (Hernandez-Pavon et al., 2012) is important to accurately separate the data into independent components.

Factors impacting the reliability of ICA

Several additional factors can impact the outcome of artifact cleaning using ICA (Fig. 5). First, independent components representing artifacts must be selected for removal by the experimenter, introducing an inherent level of subjectivity to the analysis. As such, inconsistent component selection between or even within experimenters can substantially alter the final EEG signal. Several automated and

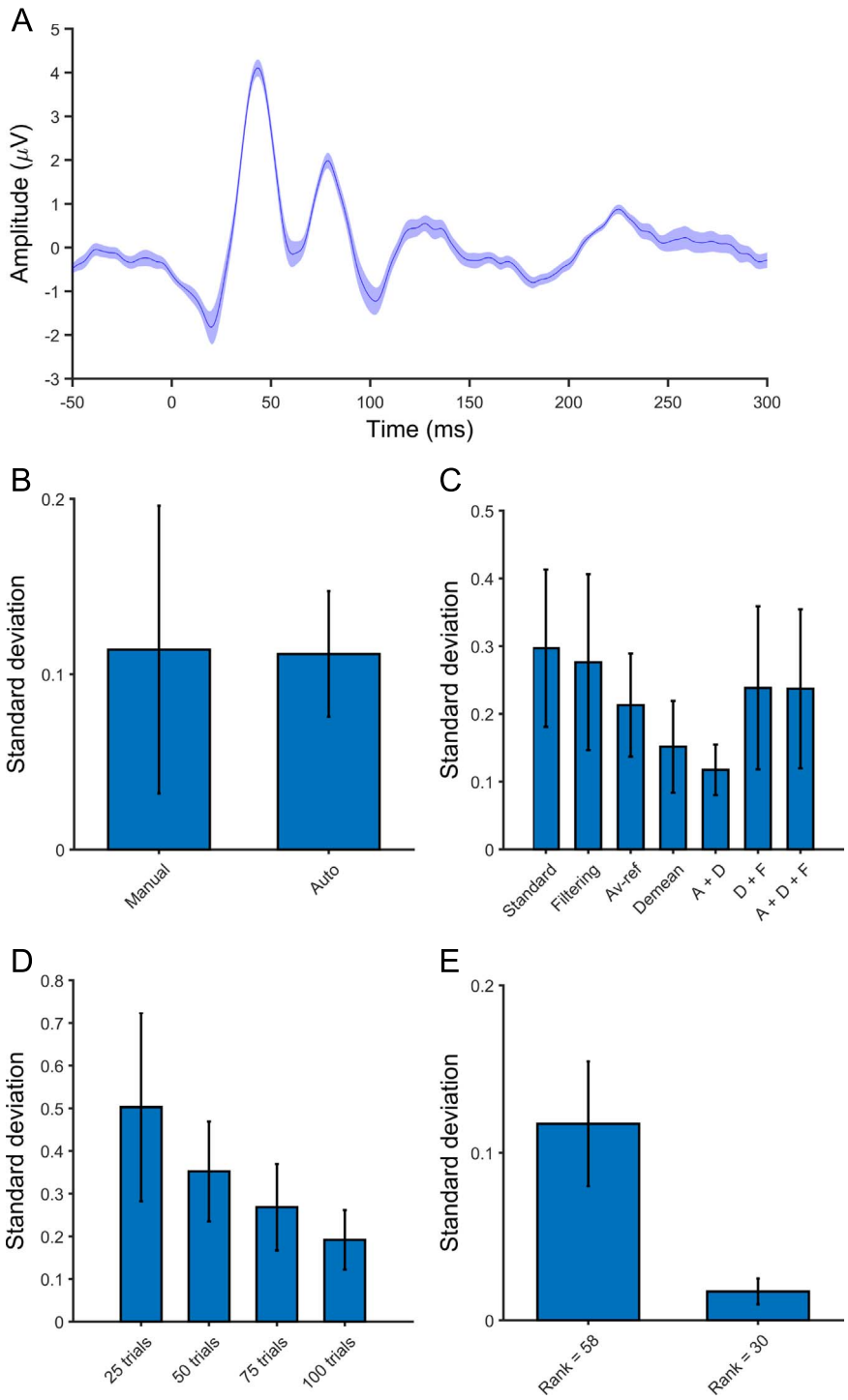

Fig. 5. Factors affecting the reliability of independent component analysis (ICA) decomposition. A) Average signal from the P3 electrode following 20 independent ICA runs over the same dataset. Artifactual components were selected using a set of heuristic thresholds (tesa_compselect function; see *Removing other artifacts caused by TMS*). The shaded area represents ± 1 standard deviation (SD), demonstrating variability in the final cleaned signal following repeated ICA runs. B) Differences in ICA variability using manual component selection compared to automated components selection with tesa_compselect function. The Y-axis represents the standard deviation in amplitude (0–500 ms) averaged across all electrodes following repeated runs of FastICA on the same data set (i.e. consistency within electrodes). Components representing artifacts were removed following each FastICA run. Error bars represent ± 1SD across electrodes (i.e. consistency between electrodes). Using rules with defined thresholds to select artifactual components (auto) reduces the variability between electrodes compared to manually selecting artifact components (manual). FastICA was run 5 times. C) Certain pre-processing steps reduce variability both within and between electrodes over repeated ICA runs. Referencing the data to the average of all electrodes (av–ref) instead of using an on-head reference and demeaning the data (demean; subtracting the average of the entire epoch) instead of baseline correcting (−500 to −10 ms) both reduce variability across FastICA runs (A+D). Interestingly, in this data band-pass (1–100 Hz) and band-stop (48–52 Hz) filtering did not improve reliability (filtering), and may even reduce the improvements in reliability gained from other pre-processing steps (A+D+F). FastICA was run 20 times and automated component selection was used to select artifactual components. D) Increasing the number of trials reduces variability within and between electrodes over repeated ICA runs. FastICA was run 20 times and automated component selection was used to select artifactual components. D) Reducing the rank of the data reduced variability within and between electrodes over repeated ICA runs. FastICA was run 20 times and automated component selection was used to select artifactual components.

semi-automated methods have been introduced (e.g. Chaumon et al., 2015), which improve reliability of selecting components to varying degrees (Fig. 5B; see *Removing other artifacts caused by TMS* for TESA approach). Second, the ICA decomposition itself will result in differing solutions when run repeated times on the same data set (Fig. 5A). This is because the statistical independence underlying ICA is learned from the data each run and most ICA algorithms are initiated randomly. The ability of ICA to return reliable decompositions is impacted by several factors, such as pre-processing (Fig. 5C), the amount of data (Fig. 5D) and the data rank (Fig. 5E). Some ICA algorithms are sensitive to low frequency drifts, and are improved by removing these drifts with high-pass filtering prior to ICA (Winkler et al., 2015). However, filtering may not always result in more consistent ICA decomposition (see Fig. 5C). Baseline correction (e.g. subtracting the average of a defined prestimulus baseline period from the entire epoch; see Appendix A) following epoching is a common pre-processing step in EEG analysis; however, this can reduce the reliability of certain ICA algorithms. For instance, Groppe et al. (2009) found that demeaning the data (e.g. subtracting the average of the entire epoch from each time point in the epoch; see appendix A) improved ICA reliability compared to removing a 100 ms baseline period (Fig. 5C). Note that demeaning (also called centering) is an important preprocessing step for ICA, and the data are automatically demeaned prior to ICA by EEGLAB. The mean is then added back to the data following ICA. Therefore, manually demeaning the data is not necessary, but can be useful to remove DC-offsets for visualising the data. Another common pre-processing step is to re-reference the data to the average of all electrodes (after excluding disconnected electrodes, which will contaminate all electrodes if not removed prior to average re-referencing) (Bigdely-Shamlo et al., 2015); however, whether this improves ICA reliability is less clear (see Fig. 5C which suggests a modest benefit that is further improved by demeaning the data). An important caveat is that removing electrodes prior to average re-referencing can result in an asymmetrical electrode distribution across the scalp, which violates the theoretical assumptions underlying average referencing. Interpolating missing electrodes (to ensure a symmetrical montage for average referencing) is not recommended prior to ICA, as this can reduce ICA reliability. As such, an alternative approach is to use an on head reference during ICA, and then interpolate missing channels and re-reference to average after ICA cleaning. In addition to pre-processing, the amount of data (i.e. number of trials) has a substantial impact on ICA reliability (Groppe et al., 2009) (Fig. 5D), as does the data rank (Hernandez-Pavon et al., 2012; Korhonen et al., 2011) (Fig. 5E). In summary, the choice of pre-processing steps and the order in which these steps are applied can have a substantial impact on the accuracy and the reliability of TMS–EEG data cleaning.

Analysis pipelines and the TMS–EEG signal analyser (TESA) extension for EEGLAB

The interaction of the TMS pulse, TMS-evoked muscle, and electrical artifacts with different EEG analysis steps has necessitated a specific order to avoid the introduction of analysis-related artifacts. Furthermore, several specialised steps are required to remove/minimise the pulse and muscle/electrical artifacts resulting from TMS. An example of one such pipeline is summarised in Table 1. There are several notable features to the pipeline order. First, band-pass and band-stop filtering is only performed once both the TMS-pulse and large amplitude TMS-evoked muscle/electrical artifacts have been removed to prevent ringing artifacts. Second, data removed around the TMS-pulse is interpolated between the pre and post removal period prior to filtering (e.g. anti-aliasing filter with downsampling or band-pass/band-stop filtering) to minimise large steps in the data which can also result in ringing artifacts following filtering. Third, the large-amplitude TMS-evoked muscle artifact is minimised/removed prior to the use of FastICA for cleaning other artifacts (blinks, eye movements, persistent muscle activity, electrode noise; step 13) in order to improve the capacity of FastICA to accurately recover component topographies. There are several approaches which have been developed/adapted to remove these large amplitude artifacts resulting from TMS while minimising distortion of underlying neural activity, several of which are included in this pipeline. Finally, the data are demeaned as opposed to baseline corrected to improve the reliability of FastICA. In this pipeline, we use FastICA for cleaning of artifacts to be consistent with our previous publications (Hernandez-Pavon et al., 2012; Korhonen et al., 2011; Rogasch et al., 2014). FastICA has the advantage of increased convergence speed compared to other ICA algorithms (Hyvärinen and Oja, 2000). However, there is ongoing debate as to which ICA algorithm performs best for EEG data (Delorme et al., 2012), and other ICA algorithms are available through EEGLAB.

The pipeline described here is similar to pipelines we have published previously (Hernandez-Pavon et al., 2012; Rogasch et al., 2014). The pipeline is also similar to that described by the FieldTrip user manual (http://www.fieldtriptoolbox.org/tutorial/tms-eeg) (Herring et al., 2015); however, there are several differences. First, we have two separate steps for removing artifacts; the first removes high amplitude early artifacts such as TMS-evoked muscle and electrical charge artifacts using one of several different methods

Table 1
An example pipeline for cleaning and analysing concurrent transcranial magnetic stimulation (TMS) and electroencephalographic (EEG) data including TESA functions.

	Analysis steps	TESA functions
1	Import data	
2	Find TMS pulse	*tesa_findpulse* or *tesa_findpulsepeak*
3	Remove bad electrodes	
4	Epoch data	
5	Demean data (or baseline correct)[a]	
6	Remove TMS pulse artifact and peaks of TMS-evoked muscle activity	*tesa_removedata*
7	Interpolate missing data around TMS pulse[b]	*tesa_interpdata*
8	Downsample data	
9	Remove bad trials	
10	Replace interpolated data around TMS pulse with constant amplitude data[c,d]	*tesa_removedata*
11	Remove large amplitude artifacts (TMS-evoked muscle, electrical, and movement artifacts)[c]	*tesa_fastica+tesa_compselect* or *tesa_edm* or *tesa_pcacompress+tesa +pcasuppress* or *tesa_detrend*
12	Interpolate missing data around TMS pulse[b,c]	*tesa_interpdata*
13	Band-pass and band-stop filter data	*tesa_filtbutter*
14	Replace interpolated data around TMS pulse with constant amplitude data[d]	*tesa_removedata*
15	Remove all other artifacts with ICA	*tesa_fastica+tesa_compselect*
16	Interpolate missing channels	
17	Re-reference to average	
18	Extract ROI and GMFA	*tesa_tepextract*
19	Find peaks	*tesa_peakanalysis*
20	Output results	*tesa_peakoutput* or *tesa_peakoutputgroup*
21	Plot the results	*tesa_plot* or *tesa_plotgroup*

N.B. Pipeline steps with no TESA functions listed have existing EEGLAB functions. ROI, region of interest; GMFA, global mean amplitude.

[a] Baseline correction can reduce ICA reliability. Demeaning the data is an alternative at this step to remove DC-offsets.

[b] Interpolating missing data following the removal of the TMS pulse is necessary prior to filtering to avoid sharp steps or transitions in the data, which can lead to ringing artifacts.

[c] These steps are only necessary if TMS-evoked muscle, electrical, or movement artifacts are present in the data.

[d] Replacing interpolated data around TMS pulse with constant amplitude data is necessary prior to ICA to improve performance.

(ICA, EDM, PCA, detrend), and the second uses FastICA to remove other artifacts such as blinks, eye movement, persistent muscle activity, and electrode noise. In the Fieldtrip pipeline, all of these artifacts are removed in one round of ICA. The reason for this two-step approach is that the presence of large amplitude artifacts such as the TMS-evoked muscle artifact can affect the decomposition accuracy of ICA when used for recovering neural activity or removing other artifacts (Hernandez-Pavon et al., 2012). In addition, removing large amplitude artifacts allows for band-pass filtering, which may further improve ICA decomposition (Winkler et al., 2015), a step which is also applied after ICA in the FieldTrip pipeline. Note that the first artifact removal step is only necessary if large amplitude artifacts are present in the data (e.g. TMS-evoked muscle, electrical charge artifacts). Second, we downsample the data, and remove bad trials and electrodes prior to ICA. These steps are applied after ICA in the Fieldtrip pipeline. Downsampling is useful to reduce the computational demand on ICA for data sampled at a high rate (> 2 kHz), but does require that the TMS pulse is removed and the missing data interpolated to prevent ringing from anti-aliasing filters. Cleaning bad trials and electrodes can also improve ICA decomposition, particularly if there are large, non-repeating artifacts present in the data (e.g. hard jaw clench, head scratch). Third, we replace removed data (e.g. around the TMS pulse artifact) with constant amplitude data (either zeros or a baseline average), as opposed to leaving a gap in the data. Adding information to the data (e.g. interpolating missing channels or time points) can alter the performance of ICA, and should therefore be avoided prior to ICA. In FieldTrip, removing data across time results in a gap in the time series, however the EEGLAB data structure does not allow gaps in time. As such, we replace this data with constant amplitude data, which avoids adding information and is therefore similar to leaving a gap. Note that constant amplitude data needs to be interpolated prior to downsampling and filtering in order to avoid steps in the data which can cause ringing artifacts (Fig. 2). However, this interpolated data should be replaced with constant amplitude data prior to subsequent rounds of ICA to avoid correlated data (see Table 1).

Although the analysis steps specific for TMS–EEG are well described in the literature, these steps are typically not included in most EEG analysis software. Furthermore, methods for removing/minimising the large amplitude artifacts such as TMS-evoked muscle and electrical charge artifacts are under active development, with no clear consensus on the most accurate methods for recovering TMS-evoked neural activity. As such, we have written a series of functions for EEGLAB called the TMS–EEG signal analyser (TESA). TESA includes functions for cleaning TMS–EEG data and performing TMS-evoked potential (TEP) peak analysis; however, the cleaning pipeline and functions are also applicable for time-frequency analysis of TEPs (already available in EEGLAB). TESA functions can be run directly from the EEGLAB GUI, thereby removing the need for any coding, or by calling the function from the command line or in a script. Importantly, EEGLAB allows for flexibility in pipeline design, enabling comparisons of different pipeline orders and different cleaning methods (e.g. for removing TMS-evoked muscle artifacts). Additional functions can easily be added to TESA as they are developed and become available. TESA functions for specific analysis steps are summarised in Table 1, and example outcomes from some of these functions are given in Fig. 6.

The TESA extension is available for download (http://nigelrogasch.github.io/TESA/) and also includes an on-line user manual with detailed instructions on using TESA (https://www.gitbook.com/book/nigelrogasch/tesa-user-manual/details). The example data used in this paper can also be downloaded (https://figshare.com/articles/TESA_example_data_and_scripts/3188800) and an example script following the analysis pipeline is available with the TESA extension (example_script_from_manual.m). An overview of the TESA functions are provided below. TESA was tested on Matlab r2015b using EEGLAB 13_5_4b.

Finding the TMS pulse

For various reasons, triggers marking the delivery of the TMS pulse can either be inaccurate or not properly recorded with the EEG signal. This should be avoided wherever possible by ensuring an adequate experimental arrangement. However, for cases where triggers are lost or inaccurate, TESA provides three functions that make use of the large amplitude and high frequency of the TMS pulse artifact to insert triggers marking a consistent time point on each TMS pulse. Each function requires the TMS pulse artifact, so they are not appropriate for systems that use sample-and-hold circuits or deblocking to avoid recording the TMS pulse artifact (e.g. the Nexstim system). All of the functions are capable of finding and marking single, paired and repetitive TMS pulses. The first function, *tesa_findpulse*, uses the first derivative of the continuous data to search for rates of change that are above a given threshold. As the frequency and amplitude of the TMS pulse artifact is 4–5 orders of magnitude larger than other signals (e.g. neural activity, persistent muscle activity or blinks), the start of this artifact is easy to differentiate. A “refractory period” is also defined, which prevents the algorithm from marking another pulse during the remainder of the pulse artifact. The second function, *tesa_findpulsepeak*, uses a series of functions (http://www.its.caltech.edu/~daw/teach.html) to find the positive and negative peaks of the TMS pulse artifact that are above 99.9% of the continuous data. Either the positive or negative aspect of the peak can be used to define the time of the TMS pulse. This function is useful if two pulses are very close together, not allowing for a long enough refractory period (e.g. < 2 ms). The *tesa_findpulsepeak* function also includes a user interface option, where users can interactively select which peaks to mark as artifacts. This is useful for selecting smaller spike artifacts that can occur with some stimulators. The third function, *tesa_fixtrigger*, is used on epoched data and is designed to correct inaccurate trigger positions or to mark paired conditions. The function uses the same derivative method as *tesa_findpulse*.

Removing the TMS pulse artifact

The *tesa_removedata* function removes data around the TMS pulse and replaces this data with constant amplitude data (either zeros or the average of a user defined prestimulus period; Fig. 6). Replacing the data with a constant amplitude avoids adding information to the data, which occurs when the data is interpolated, and is similar to leaving a gap in the data. Adding information to the data by interpolation could affect the performance of ICA, and should therefore be avoided prior to ICA. The length of data to be removed can be defined by the user. The length and timing of removed data is stored in the EEGLAB EEG structure under EEG.tmscut. Interpolation of the removed data is included as a second function to allow flexibility regarding when the interpolation is performed.

Interpolating missing data

The *tesa_interpdata* function fits either a linear or cubic model to data either side of the removal window defined with the *tesa_removedata* function and then inserts interpolated data in to this window (Fig. 6). Data is interpolated separately for each epoch and each channel. The linear model fits the first and last data point either side of removal window, whereas the cubic model fits additional data either side of the removal window, the length of which is defined by the user. The *tesa_interpdata* function requires the *tesa_removedata* function to be run first and will interpolate all data removed by this function.

Removing TMS-evoked muscle, electrical and movement artifacts

By far the most challenging aspect of TMS–EEG analysis is removing/minimising the large amplitude decay artifacts caused by

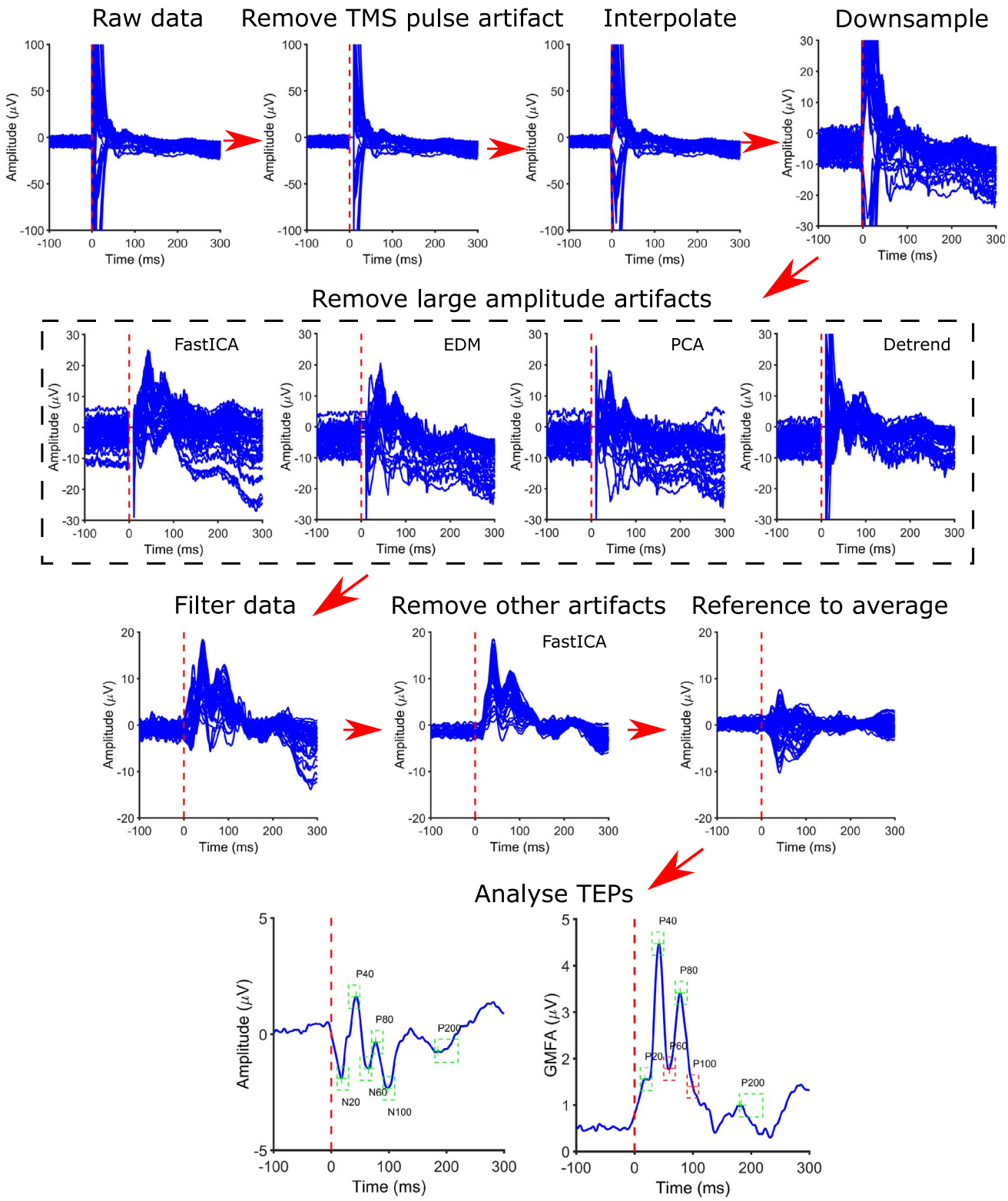

Fig. 6. An example of cleaning and analysis functions implemented using the TESA extension in EEGLAB. Raw data has been epoched around the TMS pulse and demeaned. The TMS pulse artifact is removed using *tesa_removedata* and replaced using linear interpolation with the *tesa_interpdata*. The data is downsampled to 1000 Hz using EEGLAB's *resample*. The TMS-evoked muscle artifact and electrical charge artifacts are then removed using one of several methods including: FastICA with automated component selection (*tesa_fastica*, *tesa_compselect*); enhanced deflation method (EDM; *tesa_edm*); principal component analysis (PCA; *tesa_pcasuppress*); or detrending the data by fitting and subtracting a model such as a double exponential function (*tesa_detrend*). Note that detrending the data is more appropriate for removing long decay artifacts, such as those resulting from store electrical charges. Residual TMS-evoked muscle activity can be removed with subsequent ICA. The data is then filtered using a zero-phase, fourth order Butterworth band-pass (1–100 Hz) and band-stop (48–52 Hz) filter (*tesa_filtbutter*). Other artifacts such as blinks, lateral eye movement, persistent muscle activity, and electrode noise are then removed using a second run of FastICA and automated component selection (*tesa_fastica*, *tesa_compselect*). Missing electrodes are then interpolated using EEGLAB's *interp* function and re-referenced to the average of all electrodes using *reref*. Finally, TMS-evoked potentials (TEPs) are extracted using a region of interest analysis (left) or global mean field amplitude analysis (right), and *a priori* peak amplitudes and latencies are detected (green=peak found, red=peak not found; *tesa_tepextract*, *tesa_peakanalysis*, *tesa_peakoutput*). Plots were generated using *tesa_plot*. For a full description of the pipeline, see Table 1. (For interpretation of the references to color in this figure legend, the reader is referred to the web version of this article.)

TMS-evoked muscle activity, electrical charges, and electrode movement, while leaving the underlying neural signal of interest intact. TESA provides several different approaches for addressing these types of artifacts (Fig. 5; see *Artifacts in EEG recordings following TMS* for review). As we reiterate, there is currently no consensus on the best method for correcting these artifacts.

FastICA

FastICA is one ICA algorithm commonly used for TMS–EEG data. Various different ICA algorithms including infomax and FastICA are already available in EEGLAB via the *runica* function; however, the FastICA algorithm requires a separate toolbox that can be downloaded here (http://research.ics.aalto.fi/ica/fastica/code/dlcode.shtml). In addition, TESA includes a wrapper function (*tesa_fastica*), which calls FastICA through the EEGLAB *runica* function using several settings recommended for TMS–EEG. The task of FastICA and any ICA algorithm is to estimate a separating matrix of weight vectors that gives the independent components. For FastICA, there are two different methods for finding the weight matrix, a deflation approach and a symmetric approach. In the deflation approach, the weight matrix is formed by finding the weight vectors one by one in such a way that the first found weight vector is orthogonal to the second one and so on until all the weight vectors are found and the weight matrix is formed with them. In contrast, in the symmetric approach the weight vectors are searched simultaneously for the entire weight matrix (Hyvärinen et al., 2001). The symmetric approach is reported to be more reliable and less sensitive to overlearning and is therefore recommended for TMS–EEG (Korhonen et al., 2011). Since the weight matrix cannot generally be solved in closed form, the solution is based on cost functions, also called objective functions or contrast functions. The contrast functions are conceptually simple, fast to compute, and especially very robust. The solutions of the weight matrix to ICA are found at the minima or maxima of these functions. Several possible ICA cost functions have been introduced for computing FastICA, including “tanh”, “gauss” and several others (Hyvarinen, 1997; Hyvärinen et al., 2001). There are no differences in the performance of “tanh” and “gauss” contrast functions when using FastICA to remove TMS-evoked muscle activity (Korhonen et al., 2011). For more details about the contrast functions see (Hyvarinen, 1997; Hyvärinen et al., 2001). Note that prior to FastICA, data are automatically centred and whitened; two pre-processing steps required for ICA decomposition (Hyvärinen and Oja, 2000).

EDM

In addition to FastICA, the EDM method (Korhonen et al., 2011) is implemented in TESA using the *tesa_edm* function. Components representing TMS-evoked muscle artifacts are then semi-automatically removed from the original data using an algorithm similar to *tesa_compselect* (see *Removing other artifacts caused by TMS*). The implementation of EDM in TESA differs slightly from that in the original paper in that EDM is applied to single trial data as opposed to average data. However, aside from additional computational time, this is unlikely to significantly alter the efficacy of the technique, as using ICA on single trial data instead of average data is more beneficial for any ICA algorithm since the number of samples is larger.

PCA compression

TESA implements the PCA preprocessing step, PCA compression (Hernandez-Pavon et al., 2012; Korhonen et al., 2011), in the *tesa_pcacompress* function, which uses single value decomposition for PCA and allows the user to select the number of principal components to be retained.

PCA suppression

For minimising decay artifacts using PCA, TESA includes the PCA suppression technique (Hernandez-Pavon et al., 2012), which is implemented using singular value decomposition via the *tesa_pcasuppress* function. The user is required to manually identify how many principal components to suppress based on how well the data is corrected. One difference in the implementation of the PCA-based correction algorithm in TESA is that the PCA is applied to all epoched trials, whereas PCA was applied to data averaged across trials in the original paper. This has the advantage of retaining single trial data, which can be used for additional analysis of the TMS-evoked activity. For mathematical detail of this approach see (Hernandez-Pavon et al., 2012). Note that the data analysed in Hernandez-Pavon et al. (2012) were recorded from Broca´s area and the amplitude of such data was 3 orders of magnitude larger than the brain signals; however, in data with moderate artifacts (~100 μV) it is possible to suppress artifacts right after the TMS pulse.

Detrend

In addition to blind source separation methods, TESA also includes a detrend option, which is implemented via the *tesa_detrend* function. Users can fit and subtract either a linear, exponential or double exponential model to the data following the TMS pulse. Models are fitted to each trial for each channel separately for linear models (using Matlab's *polyfit* function), and to the average across trials for exponential and double exponential models (using Matlab's *fit* function). Note that the exponential and double exponential methods require the Matlab Curve Fitting toolbox.

Removing other artifacts caused by TMS

In addition to removing large amplitude artifacts, ICA is also used to remove other artifacts such as eye movements and blinks, persistent muscle activity and electrode noise (Jung et al., 2001; Onton et al., 2006). A limitation of ICA is that the user must manually select the components representing these artifacts. This decision is informed by different component properties such as the size and timing of the component time course, the frequency distribution of the time course and the topology weights (Rogasch et al., 2014). For instance, TMS-evoked muscle activity is characterised by a large amplitude deflection in the component time course close to the TMS pulse (Fig. 1); blinks and lateral eye movements are characterised by component topologies weighted over frontal and lateral electrodes respectively (Fig. 2); persistent muscle activity is characterised by component time courses with more activity in higher frequencies (> 30 Hz; Fig. 2); and noisy electrodes are characterised by component topology weighted over single electrodes (Fig. 2). Several different automated and semi-automated approaches have been suggested for selecting artifactual components (e.g. Chaumon et al., 2015). TESA includes the *tesa_compselect* function, which uses a set of heuristic thresholding rules to classify components as either neural, TMS-evoked muscle artifacts, eye movement (blink or lateral movement), persistent muscle activity, or electrode noise. The classification can then be manually checked and altered by the user. The aim of this rule-based selection is to improve consistency in component selection within a given dataset, thereby improving within- and between-rater reliability. Classification of components is achieved by setting thresholds of characteristics unique to specific artifact types as described by Rogasch et al. (2014). A formal description of the classification rules is provided in Appendix B. Components are first sorted by the amount of variance each time course contributes to the total variance prior to classification. TMS-evoked muscle components are classified by dividing the mean absolute time course amplitude in a defined window near the TMS pulse known to include the tail of TMS-evoked muscle activity (default is 11 to

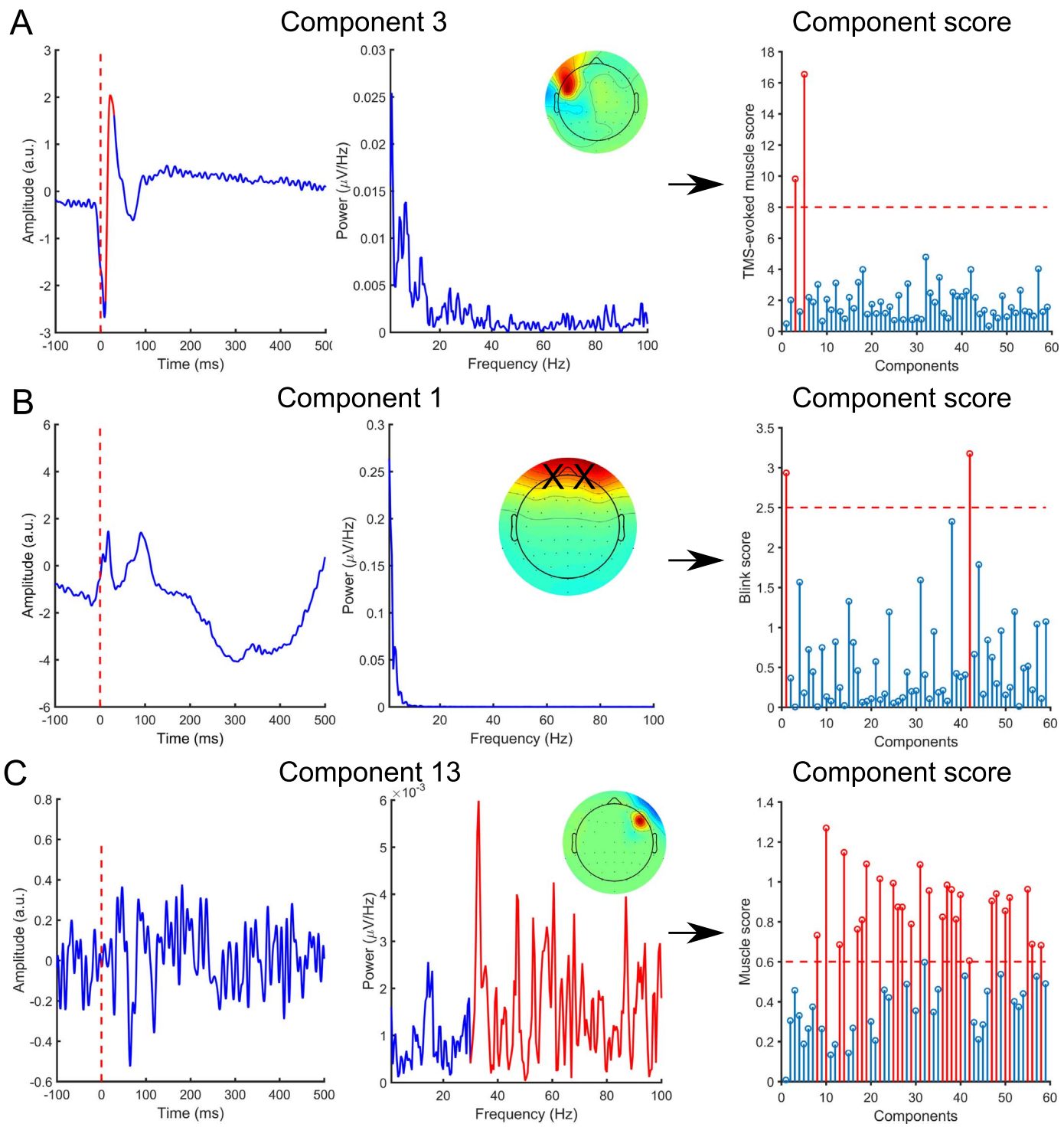

Fig. 7. Using TESA's automated component selection to categorise artifactual components. Components representing different artifact types are categorised using specific characteristics typical of the artifact, such as time course amplitude (left panel), time course frequency distribution (centre panel) and topography weights (topoplots). All components are given a score based on the characteristic of interest (right panel), and the components above a user-defined threshold (red dashed line) are categorised as artifacts (red stem plots). A) Transcranial magnetic stimulation (TMS)-evoked muscle artifacts are categorised by the time course amplitude. TMS-evoked muscle scores are calculated by dividing the mean absolute amplitude of the time course within a user-defined time window (e.g. 11–30 ms; red trace in left panel) by the mean absolute time course value across the whole epoch. Two components are characterised as TMS-evoked muscle artifacts. B) Eye blink artifacts are categorised based on the topography weights of the component. The blink score is calculated by averaging the absolute z-score corrected weights of the two electrodes closest to the eyes (FP1 and FP2, denoted by X on topoplot). Two components are characterised as blink artifacts. C) Persistent muscle artifacts are categorised based on the frequency distribution of the time course data. The muscle score is calculated by dividing the mean power within a user-defined frequency window (e.g. 30–100 Hz; red line in centre panel) by the mean power across all frequencies. 27 components are characterised as muscle artifacts. (For interpretation of the references to color in this figure legend, the reader is referred to the web version of this article.)

30 ms) by the rest of the epoch (default threshold is 8; Fig. 7A). Eye-blinks components are detected when the mean z-score corrected topology weights in the two electrodes closest to the eyes (default is FP1 and FP2) are larger than a defined value (default threshold is 2.5; Fig. 7B). Lateral eye-movement components are detected when the z-score corrected topology weights of two electrodes on the outside of the

forehead (default is F7 and F8) are larger and smaller, respectively (or *vice versa*), than a defined value (default threshold is 2). Persistent muscle components are classified by dividing the mean frequency of the time course over a defined frequency window (calculated across individual trials) by the mean of all frequencies (default threshold is 0.6; Fig. 7C). Electrode noise components are detected if the absolute z-score corrected topology weight of one electrode is greater than a defined threshold (default threshold is 4). To assess the effect of different threshold values on component classification, we compared *tesa_compselect* to manual component selection performed on 30 individuals in a previous TMS–EEG study over left dorsolateral prefrontal cortex (Rogasch et al., 2014). Three artifact categories were considered: TMS-evoked muscle activity; blinks; and noise (consisting of persistent muscle activity and electrode noise). We first compared the number of components selected for removal between manual classification, and a range of *tesa_compselect* threshold values. We then assessed the correlation between manual and automatic component classification across individuals for both the number of components classified, and the total time course variance accounted for by these components (Fig. 8). For TMS-evoked muscle artifacts, threshold values >8 classified a similar number of components to manual classification, with high correlation between component variances ($r > 0.95$). For blinks, threshold values between 2.5 and 3 classified similar numbers of components to manual classification, with good correlation between component variances ($r > 0.75$). For persistent muscle activity and electrode noise, threshold values of 0.6 and 4 respectively achieved similar results to manual classification, with good correlation between component variances ($r > 0.7$). Note that threshold values may need to be optimised for different datasets depending on experimental parameters (number of electrodes, site of stimulation, etc.). A feedback option is provided, which outputs the value used for thresholding a given artifact type for each component in the command window. Threshold values should be reported in publications where this function is used. Further examples of *tesa_compselect* are provided in the TESA user manual (https://www.gitbook.com/book/nigelrogasch/tesa-user-manual/details).

Filtering the data

Once the TMS pulse and muscle artifacts have been adequately removed (see *Artifacts introduced to TMS–EEG recordings during analysis*), band-pass and band-stop filters are often used to remove low frequency drifts, high frequency noise, and residual line noise from the EEG signal. In addition to the filtering options offered by EEGLAB, TESA includes a zero-phase Butterworth filter (band-pass and band-stop; using Matlab's *butter* and *filtfilt* functions), which is implemented using the *tesa_filtbutter* function. As mentioned previously, filtering can have unintended consequences on event-related potentials (e.g. TMS-evoked potentials) and should be used with caution (Acunzo et al., 2012; Tanner et al., 2015; VanRullen, 2011; Widmann et al., 2014; Widmann and Schröger, 2012). However, filtering can also improve the performance of ICA, increasing component dipolarity, signal to noise ratio, and neural classification using an automatic classifier (Winkler et al., 2015).

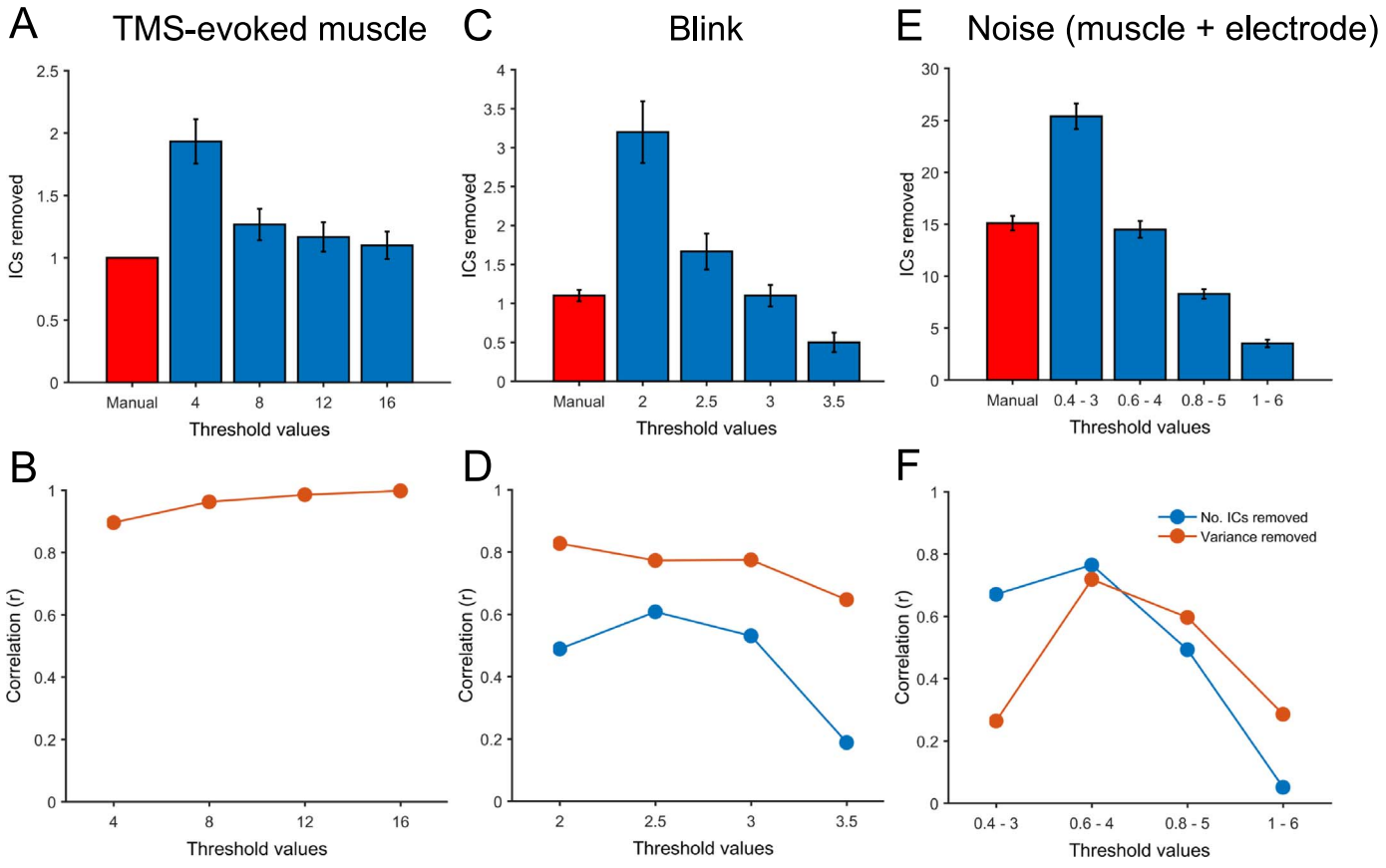

Fig. 8. Comparison between TESA's automated component selection and manual component selection. Independent component (IC) selection using TESA's *tesa_compselect* function was compared against manual IC selection performed in a previous TMS–EEG study (n=30; TMS applied to left dorsolateral prefrontal cortex) (Rogasch et al., 2014). The mean number of ICs removed (A, C, E) was compared between manual and automatic component selection for three artifact categories; TMS-evoked muscle, blinks, and noise (including persitent muscle activity and electrode noise). In addition, the correlation between manual and automatic IC selection across individuals was also compared for 1) the number of ICs removed, and 2) the total time course variance accounted for by those ICs (B, D, F). For each category, several different threshold values were used to determine optimal ranges. Note that one TMS-evoked muscle IC was removed manually for each individual, hence correlation was not performed for this artifact category. For figures E and F, the first x axis value for each data point represents the threshold value for persitent muscle artifact, and the second the threshold value for electrode noise.

TESA also allows users to implement a median filter using the *tesa_filtmedian* function. Median filters work by replacing a value with the median value taken from a given number of samples (i.e. the filter order) either side of that value (Rose et al; in press). This type of filter is useful for removing short, high frequency events such as recharge artifacts, and small spikes in the EEG data caused by electrical circuits in the TMS machine. Users should be aware that, similar to interpolation, neural data within the filtered window is not preserved and is lost. As such, median filters should only be used over small sections of data (e.g. several samples). In TESA, the user can specify the time window around an event for median filtering and the filter order.

Analysis and plotting of TMS-evoked potentials

TESA includes several basic options for analysing cleaned TMS-evoked potentials (TEPs) using either a region-of-interest (ROI) approach (i.e. data from a single electrode or averaged over a selected sub-set of electrodes) or global mean field amplitude (GMFA) analysis (Lehmann and Skrandies, 1980). TEPs are first calculated by averaging across the single trial data using the *tesa_tepextract* function. The user can define the type of analysis (ROI or GMFA) and the electrodes for inclusion in the ROI analysis; either single, multiple or all. Importantly for paired pulse studies, the *tesa_tepextract* function provides a method for subtracting the ongoing activity of the conditioning pulse from the test pulse, thereby minimising potential confounds of this activity on test pulse TEPs (Daskalakis et al., 2008; Premoli et al., 2014; Rogasch et al., 2015). The TEP data is stored in an EEG.ROI or EEG.GMFA structure. Note that multiple different ROIs can be stored simultaneously. Following TEP extraction, peaks-of-interest can be identified using the *tesa_peakanalysis* function. The user defines the latency of positive/negative peaks (e.g. N40, P60, etc.) and a time window for detection (e.g. 30–50 ms, 50–70 ms). If multiple peaks are detected in the time window specified, the user can define which peak to use, either the closest to the defined peak latency (centre) or the largest peak in the window (largest). If a peak is not detected within the window, no peak latencies are recorded. The peak information is stored within the EEG.ROI or EEG.GMFA structures. Finally, the peak amplitude and latency information can be summarised in an output table in the Matlab workspace and a figure using the *tesa_peakoutput* function. The user can define whether the output amplitudes give the absolute amplitude at the peak or an average over data points either side of the peak (e.g. ± 5 ms). Area under the curve is also available for GMFA analysis. If a peak was not detected, a NaN value is returned in the latency column. Outputs from ROI and GMFA analyses can also be obtained across a group of participants using the *tesa_peakoutputgroup* function.

ROI and GMFA analyses only represent a small subset of the ways in which TEPs can be quantified. Users can make use of other more advanced EEGLAB analysis functionality (e.g. time-frequency analysis) or output the cleaned TEP data to other open source programs such as FieldTrip (Oostenveld et al., 2011) or SPM (Litvak et al., 2011) for more principled analyses (e.g. cluster-based methods or statistical parametric mapping).

TESA also includes the *tesa_plot* function for plotting TMS-evoked data averaged across trials. During analysis, the *tesa_plot* function is useful for visually displaying the impact of different analysis steps on the data. Following use of the *tesa_tepextract* and *tesa_peakanalysis* function, *tesa_plot* can display the identified peaks and the window in which the peak was detected (Fig. 6). In addition, shaded 95% confidence interval bars can also be plotted for single electrode TEPs or ROI analyses, indicating the consistency of the evoked potentials across trials. Plots averaging across a group of participants can also be obtained using the *tesa_plotgroup* function.

Summary

Combined TMS–EEG is emerging as an important tool for evaluating cortical circuits and global brain networks. However, recovering TMS-evoked neural activity from the numerous artifacts associated with combined TMS–EEG is challenging. The TESA extension builds on existing EEGLAB functionality to provide a basic framework for cleaning and analysing TMS–EEG data. Importantly, the extension provides access to several state-of-the-art methods for removing the large amplitude muscle and decay artifacts, while recovering underlying neural activity. The field of TMS–EEG analysis is rapidly evolving. By making this extension open source, we hope to improve consistency and transparency in reporting the steps used to analyse TMS–EEG data across the brain stimulation field. We also invite other researchers to contribute new and improved approaches for cleaning and analysing TMS–EEG data as they become available by sharing their code in TESA (code contributions can be made using github: https://github.com/nigelrogasch/TESA).

Conflicts of interest

PBF has received equipment for research from MagVenture A/S, Medtronic Ltd, Cervel Neurotech and Brainsway Ltd and funding for research from Neuronetics and Cervel Neurotech. He is on the scientific advisory board for Bionomics Ltd. There are no further conflicts.

Acknowledgement

We wish to thank Prof. Ulf Ziemann, Dr. Florian Müller-Dahlhaus, Dr. Carl Zipser and Ghazal Darmani for assistance in collecting the example data and Dr. Ben Fulcher for advice on open source software. NCR is supported by a research fellowship from the National Health and Medical Research Council of Australia (1072057). PBF is supported by a NHMRC Practitioner Fellowship (1078567). FF receives funding from Natural Sciences and Engineering Research Council of Canada (RGPIN-2015-05783).

Appendix A

Baseline correction is a typical EEG pre-processing step, which involves subtracting the mean of predefined baseline period from all time points in the epoch

$$\widetilde{S}_t = S_t - \left(\frac{1}{b_2 - b_1} \sum_{t=b_1}^{b_2} S_t \right), \tag{1}$$

where S_t is the EEG signal from a given electrode, t is a time index, b_1 and b_2 ($>b_1$) are time points designating a baseline period, and $\widetilde{S}_t$ is the corrected EEG signal.

Demeaning the data involves subtracting the mean of the entire epoch from each time point in the epoch

$$\widetilde{S}_t = S_t - \left(\frac{1}{N}\sum_{t=1}^{N} S_t\right), \tag{2}$$

where N is the total number of time points.

Appendix B

The following rules are applied to classify independent components as artifacts using the *tesa_compselect* function.

TMS-evoked muscle activity

A component is classified as a TMS-evoked muscle artifact when

$$\frac{1}{b_2 - b_1}\sum_{t=b_1}^{b_2} |S_t| \Big/ \frac{1}{N}\sum_{t=1}^{N} |S_t| > T, \tag{3}$$

where S_t is the component time course averaged across trials, t is a time index, b_1 and b_2 ($>b_1$) are time points designating a period where TMS-evoked muscle activity is expected, and T is a threshold value.

Eye blink

A component is classified as an eye blink artifact when

$$\left|\frac{1}{2}[(w_{e1} - \overline{w})/\sigma_w + (w_{e2} - \overline{w})/\sigma_w]\right| > T, \tag{4}$$

where $\overline{w}$ is the mean weight across all scalp electrodes of a component, σ_w is the standard deviation of weights across all scalp electrodes, and w_{e1} and w_{e2} are the two electrodes closest to the eyes.

Lateral eye movement

A component is classified as a lateral eye movement artifact when

$$(w_{e1} - \overline{w})/\sigma_w > T \tag{5}$$

and

$$(w_{e2} - \overline{w})/\sigma_w < -T, \tag{6}$$

for any two electrodes w_{e1} and w_{e2}, where w_{e1} and w_{e2} are the electrodes located lateral to the eyes.

Persistent muscle activity

A component is classified as a persistent muscle activity artifact when

$$\frac{1}{x_2 - x_1}\sum_{f=x_1}^{x_2} |Y_f| \Big/ \frac{1}{N}\sum_{f=1}^{N} |Y_f| > T, \tag{7}$$

where Y_f is the Fourier transformation of the time-domain component signal, and x_1 and x_2 ($>x_1$) are frequencies between which persistent muscle activity is expected.

Electrode noise

A component is classified as an electrode noise artifact when

$$|(w_e - \overline{w})/\sigma_w| > T, \tag{8}$$

where w_e is any given electrode.

References

Acunzo, D.J., MacKenzie, G., van Rossum, M.C.W., 2012. Systematic biases in early ERP and ERF components as a result of high-pass filtering. J. Neurosci. Methods 209, 212–218.

Amassian, V.E., Cracco, R.Q., Maccabee, P.J., Cracco, J.B., 1992. Cerebello-frontal cortical projections in humans studied with the magnetic coil. Electroencephalogr. Clin. Neurophysiol. 85, 265–272.

Berg, P., Scherg, M., 1994. A multiple source approach to the correction of eye artifacts. Electroencephalogr. Clin. Neurophysiol. 90, 229–241.

Bergmann, T.O., Mölle, M., Schmidt, M. a, Lindner, C., Marshall, L., Born, J., Siebner, H.R., 2016. Combining non-invasive transcranial brain stimulation with neuroimaging and electrophysiology: current approaches and future perspectives. NeuroImage.

Bergmann, T.O., Mölle, M., Schmidt, M. a, Lindner, C., Marshall, L., Born, J., Siebner, H.R., 2012. EEG-guided transcranial magnetic stimulation reveals rapid shifts in motor cortical excitability during the human sleep slow oscillationJ. Neurosci. 32, 243–253.

Bigdely-Shamlo, N., Mullen, T., Kothe, C., Su, K.-M., Robbins, K.A., 2015. The PREP pipeline: standardized preprocessing for large-scale EEG analysis. Front. Neuroinform. 9, 16.

Bonato, C., Miniussi, C., Rossini, P.M., 2006. Transcranial magnetic stimulation and cortical evoked potentials: a TMS/EEG co-registration study. Clin. Neurophysiol. 117, 1699–1707.

Chaumon, M., Bishop, D.V.M., Busch, Na, 2015. A practical guide to the selection of independent components of the electroencephalogram for artifact correction. J. Neurosci. Methods.

Cracco, R.Q., Amassian, V.E., Maccabee, P.J., Cracco, J.B., 1989. Comparison of human transcallosal responses evoked by magnetic coil and electrical stimulation. Electroencephalogr. Clin. Neurophysiol. 74, 417–424.

Daskalakis, Z.J., Farzan, F., Barr, M.S., Maller, J.J., Chen, R., Fitzgerald, P.B., 2008. Long-interval cortical inhibition from the dorsolateral prefrontal cortex: a TMS-EEG study. Neuropsychopharmacology 33, 2860–2869.

Delorme, A., Makeig, S., 2004. EEGLAB: an open source toolbox for analysis of single-trial EEG dynamics including independent component analysis. J. Neurosci. Methods 134, 9–21.

Delorme, A., Palmer, J., Onton, J., Oostenveld, R., Makeig, S., 2012. Independent EEG sources are dipolar. PLoS One, 7.

Fitzgerald, P.B., Daskalakis, Z.J., Hoy, K., Farzan, F., Upton, D.J., Cooper, N.R., Maller, J.J., 2008. Cortical inhibition in motor and non-motor regions: a combined TMS-EEG study. Clin. EEG Neurosci. 39, 112–117.

Groppe, D.M., Makeig, S., Kutas, M., 2009. Identifying reliable independent components via split-half comparisons. NeuroImage 45, 1199–1211.

Hamidi, M., Slagter, H. a, Tononi, G., Postle, B.R., 2010. Brain responses evoked by high-frequency repetitive transcranial magnetic stimulation: an event-related potential study. Brain Stimul. 3, 2–14.

Hernandez-Pavon, J.C., Metsomaa, J., Mutanen, T., Stenroos, M., Mäki, H., Ilmoniemi, R.J., Sarvas, J., 2012. Uncovering neural independent components from highly artifactual TMS-evoked EEG data. J. Neurosci. Methods 209, 144–157.

Herring, J.D., Thut, G., Jensen, O., Bergmann, T.O., 2015. Attention modulates TMS-locked alpha oscillations in the visual cortex. J. Neurosci. 35, 14435–14447.

Hyvarinen, A., 1997. A family of fixed-point algorithms for independent component analysis. In: Proceedings of the 1997 IEEE International Conference on Acoustics,

Speech, and Signal Processing. IEEE Comput. Soc. Press, pp. 3917–3920.
Hyvärinen, A., Karhunen, J., Oja, E., 2001. Independent Component Analysis. John Wiley & Sons, Inc, New York, USA.
Hyvärinen, a, Oja, E., 2000. Independent component analysis: algorithms and applications. Neural Netw. 13, 411–430.
Ilmoniemi, R.J., Hernandez-Pavon, J.C., Makela, N.N., Metsomaa, J., Mutanen, T.P., Stenroos, M., Sarvas, J., 2015. Dealing with artifacts in TMS-evoked EEG. In: Proceedings of Annu. Int. Conf. IEEE Eng. Med. Biol. Soc. IEEE Eng. Med. Biol. Soc. Annu. Conf. 2015, pp. 230–3.
Ilmoniemi, R.J., Kicić, D., 2010. Methodology for combined TMS and EEG. Brain Topogr. 22, 233–248.
Ilmoniemi, R.J., Virtanen, J., Ruohonen, J., Karhu, J., Aronen, H.J., Näätänen, R., Katila, T., 1997. Neuronal responses to magnetic stimulation reveal cortical reactivity and connectivity. NeuroReport 8, 3537–3540.
Izumi, S., Takase, M., Arita, M., Masakado, Y., Kimura, A., Chino, N., 1997. Transcranial magnetic stimulation-induced changes in EEG and responses recorded from the scalp of healthy humans. Electroencephalogr. Clin. Neurophysiol. 103, 319–322.
Julkunen, P., Pääkkönen, a, Hukkanen, T., Könönen, M., Tiihonen, P., Vanhatalo, S., Karhu, J., 2008. Efficient reduction of stimulus artefact in TMS-EEG by epithelial short-circuiting by mini-punctures. Clin. Neurophysiol. 119, 475–481.
Jung, T.-P., Makeig, S., McKeown, M.J., Bell, A.J., Lee, T.-W., Sejnowski, T.J., 2001. Imaging Brain dynamics using independent component analysis. Proc. IEEE. Inst. Electr. Electron. Eng. 89, 1107–1122.
Kähkönen, S., Wilenius, J., Nikulin, V.V., Ollikainen, M., Ilmoniemi, R.J., 2003. Alcohol reduces prefrontal cortical excitability in humans: a combined TMS and EEG study. Neuropsychopharmacology 28, 747–754.
Korhonen, R.J., Hernandez-Pavon, J.C., Metsomaa, J., Mäki, H., Ilmoniemi, R.J., Sarvas, J., 2011. Removal of large muscle artifacts from transcranial magnetic stimulation-evoked EEG by independent component analysis. Med. Biol. Eng. Comput. 49, 397–407.
Lehmann, D., Skrandies, W., 1980. Reference-free identification of components of checkerboard-evoked multichannel potential fields. Electroencephalogr. Clin. Neurophysiol. 48, 609–621.
Litvak, V., Komssi, S., Scherg, M., Hoechstetter, K., Classen, J., Zaaroor, M., Pratt, H., Kahkonen, S., 2007. Artifact correction and source analysis of early electroencephalographic responses evoked by transcranial magnetic stimulation over primary motor cortex. NeuroImage 37, 56–70.
Litvak, V., Mattout, J., Kiebel, S., Phillips, C., Henson, R., Kilner, J., Barnes, G., Oostenveld, R., Daunizeau, J., Flandin, G., Penny, W., Friston, K., 2011. EEG and MEG data analysis in SPM8. Comput. Intell. Neurosci. 2011, 852961.
Luck, S.J., 2005. An Introduction to the Event-related Potential Technique. MIT Press, Cambridge, MA.
Lyzhko, E., Hamid, L., Makhortykh, S., Moliadze, V., Siniatchkin, M., 2015. Comparison of three ICA algorithms for ocular artifact removal from TMS-EEG recordings. In: Proceedings of Annu. International Conference IEEE Eng. Med. Biol. Soc. IEEE Eng. Med. Biol. Soc. Annu. Conference 2015, 1926–1929
Makeig, S., Jung, T.P., Bell, a J., Ghahremani, D., Sejnowski, T.J., 1997. Blind separation of auditory event-related brain responses into independent components. Proc. Natl. Acad. Sci. USA 94, 10979–10984.
Mäki, H., Ilmoniemi, R.J., 2011. Projecting out muscle artifacts from TMS-evoked EEG. NeuroImage 54, 2706–2710.
Massimini, M., Ferrarelli, F., Huber, R., Esser, S.K., Singh, H., Tononi, G., 2005. Breakdown of cortical effective connectivity during sleep. Science 309, 2228–2232.
McMenamin, B.W., Shackman, A.J., Maxwell, J.S., Bachhuber, D.R.W., Koppenhaver, A.M., Greischar, L.L., Davidson, R.J., 2010. Validation of ICA-based myogenic artifact correction for scalp and source-localized EEG. NeuroImage 49, 2416–2432.
Morbidi, F., Garulli, A., Prattichizzo, D., Rizzo, C., Manganotti, P., Rossi, S., 2007. Off-line removal of TMS-induced artifacts on human electroencephalography by Kalman filter. J. Neurosci. Methods 162, 293–302.
Mutanen, T., Mäki, H., Ilmoniemi, R.J., 2013. The effect of stimulus parameters on TMS-EEG muscle artifacts. Brain Stimul. 6, 371–376.
Mutanen, T.P., Kukkonen, M., Nieminen, J.O., Stenroos, M., Sarvas, J., Ilmoniemi, R.J., 2016. Recovering TMS-evoked EEG responses masked by muscle artifacts. NeuroImage 139, 157–166.
Nikouline, V., Ruohonen, J., Ilmoniemi, R.J., 1999. The role of the coil click in TMS assessed with simultaneous EEG. Clin. Neurophysiol. 110, 1325–1328.
Onton, J., Westerfield, M., Townsend, J., Makeig, S., 2006. Imaging human EEG dynamics using independent component analysis. Neurosci. Biobehav. Rev. 30, 808–822.
Oostenveld, R., Fries, P., Maris, E., Schoffelen, J.-M., 2011. FieldTrip: open source software for advanced analysis of MEG, EEG, and invasive electrophysiological data. Comput. Intell. Neurosci. 2011, 156869.
Paus, T., Sipila, P.K., Strafella, a P., 2001. Synchronization of neuronal activity in the human primary motor cortex by transcranial magnetic stimulation: an EEG study. J. Neurophysiol. 86, 1983–1990.
Plöchl, M., Ossandón, J.P., König, P., 2012. Combining EEG and eye tracking: identification, characterization, and correction of eye movement artifacts in electroencephalographic data. Front. Hum. Neurosci. 6, 278.
Premoli, I., Rivolta, D., Espenhahn, S., Castellanos, N., Belardinelli, P., Ziemann, U., Müller-Dahlhaus, F., 2014. Characterization of GABAB-receptor mediated neurotransmission in the human cortex by paired-pulse TMS-EEG. NeuroImage 103, 152–162.
Rogasch, N.C., Daskalakis, Z.J., Fitzgerald, P.B., 2015. Cortical inhibition of distinct mechanisms in the dorsolateral prefrontal cortex is related to working memory performance: a TMS–EEG studyCortex 64, 68–77.
Rogasch, N.C., Fitzgerald, P.B., 2013. Assessing cortical network properties using TMS-EEG. Hum. Brain Mapp. 34, 1652–1669.
Rogasch, N.C., Thomson, R.H., Daskalakis, Z.J., Fitzgerald, P.B., 2013. Short-latency artifacts associated with concurrent TMS-EEG. Brain Stimul. (6), 868–876.
Rogasch, N.C., Thomson, R.H., Farzan, F., Fitzgibbon, B.M., Bailey, N.W., Hernandez-Pavon, J.C., Daskalakis, Z.J., Fitzgerald, P.B., 2014. Removing artefacts from TMS-EEG recordings using independent component analysis: importance for assessing prefrontal and motor cortex network properties. NeuroImage 101, 425–439.
N.S. Rose J. LaRocque A. Riggall O. Gosseries M.J. Starrett E.E. Meyering B.R. Postle (in press). Reactivation of latent working memories with transcranial magnetic stimulation. Science
Sekiguchi, H., Takeuchi, S., Kadota, H., Kohno, Y., Nakajima, Y., 2011. TMS-induced artifacts on EEG can be reduced by rearrangement of the electrode's lead wire before recording. Clin. Neurophysiol. 122, 984–990.
Siebner, H.R., Bergmann, T.O., Bestmann, S., Massimini, M., Johansen-Berg, H., Mochizuki, H., Bohning, D.E., Boorman, E.D., Groppa, S., Miniussi, C., Pascual-Leone, A., Huber, R., Taylor, P.C.J., Ilmoniemi, R.J., De Gennaro, L., Strafella, A.P., Kähkönen, S., Klöppel, S., Frisoni, G.B., George, M.S., Hallett, M., Brandt, S. a, Rushworth, M.F., Ziemann, U., Rothwell, J.C., Ward, N., Cohen, L.G., Baudewig, J., Paus, T., Ugawa, Y., Rossini, P.M., 2009. Consensus paper: combining transcranial stimulation with neuroimaging. Brain Stimul. 2, 58–80.
Spieser, L., Meziane, H.B., Bonnard, M., 2010. Cortical mechanisms underlying stretch reflex adaptation to intention: a combined EEG-TMS study. NeuroImage 52, 316–325.
Tanner, D., Morgan-Short, K., Luck, S.J., 2015. How inappropriate high-pass filters can produce artifactual effects and incorrect conclusions in ERP studies of language and cognition. Psychophysiology 52, 997–1009.
ter Braack, E.M., de Jonge, B., van Putten, M.J. a M., 2013. Reduction of TMS induced artifacts in EEG using principal component analysis. IEEE Trans. Neural Syst. Rehabil. Eng. 21, 376–382.
ter Braack, E.M., de Vos, C.C., van Putten, M.J. a M., 2015. Masking the Auditory Evoked Potential in TMS-EEG: a Comparison of Various Methods. Brain Topogr. 28, 520–528.
Thut, G., Veniero, D., Romei, V., Miniussi, C., Schyns, P., Gross, J., 2011. Rhythmic TMS causes local entrainment of natural oscillatory signatures. Curr. Biol. 21, 1176–1185.
Tiitinen, H., Virtanen, J., Ilmoniemi, R.J., Kamppuri, J., Ollikainen, M., Ruohonen, J., Näätänen, R., 1999. Separation of contamination caused by coil clicks from responses elicited by transcranial magnetic stimulation. Clin. Neurophysiol. 110, 982–985.
Uusitalo, M. a, Ilmoniemi, R.J., 1997. Signal-space projection method for separating MEG or EEG into components. Med. Biol. Eng. Comput. 35, 135–140.
VanRullen, R., 2011. Four common conceptual fallacies in mapping the time course of recognition. Front. Psychol. 2, 1–6.
Veniero, D., Bortoletto, M., Miniussi, C., 2009. TMS-EEG co-registration: on TMS-induced artifact. Clin. Neurophysiol. 120, 1392–1399.
Verhagen, L., Dijkerman, H.C., Medendorp, W.P., Toni, I., 2012. Cortical Dynamics of Sensorimotor Integration during Grasp Planning. J. Neurosci. 32, 4508–4519.
Vernet, M., Brem, A., Farzan, F., 2014. ScienceDirect synchronous and opposite roles of the parietal and prefrontal cortices in bistable perception: a double-coil TMS e EEG study. Cortex 64, 78–88.
Virtanen, J., Ruohonen, J., Näätänen, R., Ilmoniemi, R.J., 1999. Instrumentation for the measurement of electric brain responses to transcranial magnetic stimulation. Med. Biol. Eng. Comput. 37, 322–326.
Widmann, A., Schröger, E., 2012. Filter effects and filter artifacts in the analysis of electrophysiological data. Front. Psychol. 3, 1–5.
Widmann, A., Schröger, E., Maess, B., 2014. Digital filter design for electrophysiological data - a practical approach. J. Neurosci. Methods 250, 34–46.
Winkler, I., Debener, S., Muller, K.R., Tangermann, M., 2015. On the influence of high-pass filtering on ICA-based artifact reduction in EEG-ERP. Proc. Annu. Int. Conf. IEEE Eng. Med. Biol. Soc. EMBS 2015-Novemvet, pp. 4101–4105.